CHAPTER 1.5

Surface Chemical Control in Flotation and Leaching

Roger St.C. Smart, Andrea R. Gerson, and Brian R. Hart

This chapter provides a guide to plant metallurgists seeking to improve recovery and/or selectivity in froth flotation and in recovery from leaching where this is limited by mineralogy and surface chemistry of mineral phases. It aims to provide a strategy for recognition of these limitations, to provide advice on strategic analysis of the limiting mineralogy and/or surface chemistry, and to offer potential changes to operation suggested by this analysis. Some of the information used here is derived from previous compilations of research from many authors and mineral processing laboratories that have provided the basis for the development of this strategy and operational control. In particular, "Innovations in Measurement of Mineral Structure and Surface Chemistry in Flotation: Past, Present and Future" (Smart et al. 2014a) has provided much of the basic information on the analysis techniques. For more detailed references, other compilations (Smart et al. 2003a, 2003b, 2007, 2014b; Hart and Dimov 2011; Chandra and Gerson 2006) contain all the references to the development of the strategy described in this chapter. The focus here is on using these techniques with examples from plant analyses to suggest operational improvement.

WHEN TO USE MINERALOGY AND SURFACE CHEMICAL ANALYSIS: DIAGNOSIS OF LIMITING SPECIES

Froth Flotation

Losses of value in froth flotation have multiple possible causes, as the multivariable froth flotation models illustrate (e.g., JKTech 2011; Ralston et al. 2007). In this context, it is useful to identify some of these complexities that will be relevant to later discussion, including

- The extent of liberation of individual mineral phases by grinding or, conversely, the extent of remaining composite particles;
- The presence of a wide range of particle sizes in the ground sulfide ores;
- Chemical alteration of the surface layers of the sulfide minerals induced by oxidation reactions in the pulp solution;
- Galvanic interactions between different sulfide minerals to produce different reaction products on the mineral surfaces;
- Reaction and dissolution of gangue (e.g., oxide, silicate) minerals releasing ionic species interfering with surface chemical control;
- Interaction between particles in the form of aggregates and flocs;
- The presence of colloidal precipitates arising from dissolution of the sulfide minerals, gangue minerals, and grinding media;
- The mechanism of adsorption of reagents onto specific surface sites; and
- Competitive adsorption between oxidation products, conditioning reagents, and collector reagents.

Liberation and liberation analysis, discussed in detail in Chapter 1.4, "Ore Liberation Analysis," is normally the first consideration for improving flotation performance (Johnson and Munro 2002) by optimizing the size profile by mineral. The techniques of Quantitative Evaluation of Minerals by Scanning Electron Microscopy (QEMSCAN), mineral liberation analysis (MLA), and X-ray diffraction (XRD) are well established in routine use to define both valuable and gangue minerals in an ore to be processed. Some examples can be found in Lastra (2007). Three levels of analysis should be considered: mineral recovery–size relationships for all valuable minerals and any naturally floatable, hydrophobic gangue minerals (e.g., talc); mineral recovery–liberation–size relationships after grinding (liberation analysis); and surface analysis of relevant minerals in the defined size fractions after grinding. The operational basis of the first two levels of analysis are the subject of other chapters in this handbook. The third level is the subject of this chapter concerning analysis of these minerals after grinding and in subsequent flotation stages.

In operational terms, mineralogical interferences and surface chemical control tend to be considered after most other operating variables have been adjusted with fixed reagent doses and further improvement is still required or when a

Roger St.C. Smart, Emeritus Professor & Senior Consultant, Univ. of South Australia & Blue Minerals Consultancy, Mawson Lakes, South Australia, Australia
Andrea R. Gerson, Professor & Managing Director, Blue Minerals Consultancy, Middleton, South Australia, Australia
Brian R. Hart, Adjunct Professor & Senior Research Scientist, Univ. of Western Ontario & Surface Science Western, London, Ontario, Canada

deleterious change has occurred without explanation. After liberation, pulp density, bubble size, gas flow and holdup, agitation, froth control, and other cell parameters have been adjusted with no further improvement, it is the attachment of collector-conditioned mineral particles to bubbles and the stability of this bubble–particle attachment, in both pulp and froth phases, that determines recovery and grade. If this is still unacceptable, the reasons for losses likely lie in the mineralogy and surface chemistry of the conditioned feed. In froth flotation, it is the chemistry of the top few monolayers of different mineral surfaces that determine the recovery and grade in operation. The chemistry of these surface monolayers is determined by reaction of the mineral phases in pulp (e.g., oxidation of sulfides, selective leaching of different minerals) by interferences arising from fine particle or precipitate attachment and by addition of collectors and other reagents, including activators and depressants. The collector is designed to adsorb to the valuable mineral particle surfaces, making them selectively hydrophobic, so that these surfaces prefer to attach to bubbles (displacing water to expose gas–solid interfaces) rather than to water molecules. The surface of all other minerals are assumed or designed (by depressant addition) to be hydrophilic. In reality, however, the surface of each individual mineral particle in the flotation pulp is a complex, distinctly nonuniform array of precipitates (e.g., calcium sulfate or $CaSO_4$, amorphous aluminosilicates), oxidation products from sulfides (i.e., oxyhydroxides, oxy-sulfur species), adsorbed ions, and attached fine and ultrafine particles of other mineral phases, including clays—all hydrophilic surface species—with hydrophobic collector and metal-collector complexes. In feed mineralogy, in addition to particle size distribution and liberation of value minerals normally measured, interference from rapidly soluble minerals, clays, and amorphous phases can seriously compromise recovery and grade. Bubble attachment is therefore largely dependent on the ratio of hydrophobic to hydrophilic surface species on individual mineral surfaces. If this ratio is too low for the value mineral particles, recovery will be low and flotation kinetics too slow. This ratio varies widely between different particles of the same mineral, requiring statistical analysis, and some nonvalue mineral phases will also have adsorbed hydrophobic collector in some form, contributing to gangue recovery and lower grades.

This hydrophobic/hydrophilic ratio may seem an esoteric measure to plant operators, but it has been shown to determine whether particles of both value and gangue report, correctly or incorrectly, to concentrate and tail. To understand and improve poor flotation recovery, it is first necessary to know whether this is being caused by unrecognized interferences in the mineralogy of the feed or poor hydrophobic/hydrophilic conditioning of the value mineral surfaces or inadvertent hydrophobic conditioning of gangue minerals. It is then possible to define the reasons for this before changes to mechanical or chemical conditioning can be usefully made.

A complete strategy has been developed for identification of the reasons for losses in recovery and/or grade due to changes or complications in mineralogy and in mineral surface conditioning, and their subsequent correction. The principle of this strategy involves comparison of surface chemistry of selected mineral phases (value and misreporting gangue) between flotation feed, concentrate, and tail. Ideally, comparison should be made between these samples from the plant in normal operation (baseline) and the same set of samples in poor operation for root-cause analysis. This is not usually possible because baseline surface analysis is not often done. Instead, it is used more in troubleshooting mode when an unexplained loss of recovery or grade has occurred. In this mode, it is first essential to fully define the mineralogy to identify interference from rapidly soluble minerals, clays, and amorphous phases. To understand and improve poor flotation recovery where it is due to surface chemistry, it is the variation of specific hydrophobic and hydrophilic species by particle and as a statistical distribution between different mineral phases across a flotation circuit (e.g., feed, successive concentrates, tails) that one needs to know. This requires surface analysis of a large number of particles with high spatial resolution and chemical speciation. This is a difficult proposition, but surface analysis has come a long way toward this goal. A sequence of measurements using this strategy, with examples of diagnosis and outcomes, is outlined in this chapter.

Leaching Operations

This strategy is equally applicable to recovery of metals by hydrometallurgical leaching, where leach kinetics and selectivity can be cost limiting. Rate-determining surface species and surface layers forming during leaching may limit access of reactants to the surface and of reaction products to the solution. They may also indicate the mechanism of the reaction pathway for optimization of operation. The limiting actions of complexants, oxidation products, fine gangue interference, precipitates as colloidal products, and thick surface layers (amorphous and crystalline) need to be defined before the subprocesses requiring change can be usefully addressed. In leaching operations, the analytical principle involves comparison of surface chemistry of selected minerals taken during the leach progress and, where possible, comparison of good and poor leach operation.

METHODS OF MINERALOGICAL AND SURFACE ANALYSIS

This section outlines the analytical techniques used to diagnose limiting mineralogical and surface chemical factors and the approach the chapter authors used in their application to plant operation.

Sampling from Operating Slurries

Ideally, samples are collected directly from the operating plant using rigorous sampling protocols to ensure that the surface chemistry is as close as possible to that in the flotation or leach circuit at the time of sampling. They may also be collected from lab floats or leach trials using the same protocol where these are being used to test improved processing. Comparison of the feeds, concentrates, and tails or successive leach samples, where possible, between conditions that give varied recovery and grades is a more direct way to recognize the mineralogical or surface chemical factors differentiating in the flotation selectivity or kinetic leach profiles. This requires that the sample is representative of the stream, does not oxidize or react in the sample tube (i.e., is frozen) after sampling, and that these conditions are maintained in delivery to the lab and analytical instruments. In the flotation plant, the feed is normally sampled after reagent addition, the concentrates are sampled by cutting the lip of the cell or in the launder, and the tails are sampled from the final cell using a splitter box in each case. Protocols for these requirements have been developed and verified by correlation with flotation response over more than two decades.

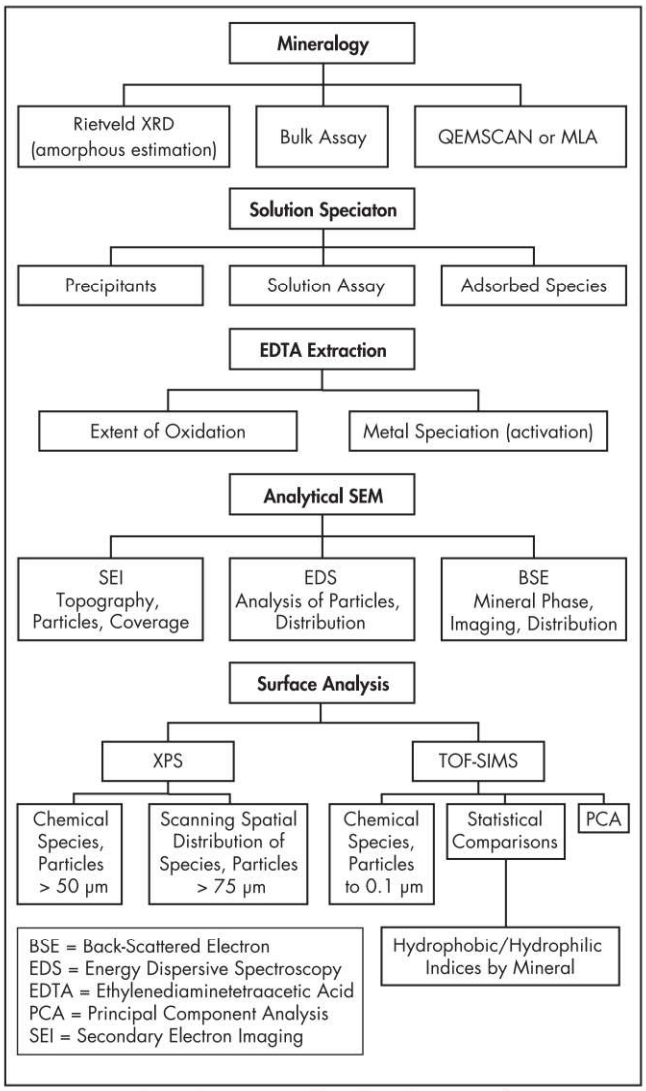

Figure 1 Analytical sequence for identification of mineralogical and surface chemical factors that may be limiting recovery and grade in flotation and leaching operations

The essential steps for sampling are described in Smart et al. (2007). In all cases, representative subsamples should be collected in a specimen tube (10–20 mL polypropylene vials), deoxygenated by bubbling argon (e.g., Ar/H_2 welding gas) or oxygen-free N_2 through the tube for 5 minutes, then closed with polytetrafluoroethylene (plumbers') tape and tightly screw capped. The tube should then be immediately frozen in liquid N_2 (or in a freezer if N_2 is not available on-site). The vial should not be completely filled to the top because it will split when frozen. Each vial should be clearly marked with a permanent marker. The pH and Eh of each stream (feed, concentrate, and tails) must be recorded at the time of sampling and supplied with the frozen samples.

It is essential for the sample to remain frozen until analysis. The sample can be delivered in a cryogenic container or, if delivery will be less than 48 hours, in a polystyrene six-pack cooler box. A cryogenic container licensed for international transport of liquid-nitrogen-frozen specimens is usually supplied by the lab conducting the surface analysis. It can maintain a temperature of less than −150°C for up to 21 days. The cooler box, if used, can be packed with freezer packs or, even better, Carbice (solid carbon dioxide, or CO_2) around the sample tubes and sealed with tape. The frozen sample vials should be transferred to the freight office immediately after freezing for fastest possible transfer to the lab. The key to success with this analysis and diagnosis is engagement from the outset with a professional surface analytical lab working with minerals processing companies. They will provide advice and support around sampling, containers, shipping, interpreting, and acting on results.

At the lab, the sample is thawed and, if necessary, the supernatant solution replaced by decantation with MilliQ water adjusted to the initial plant pH using either sodium hydroxide (NaOH) or hydrochloric acid (HCl). Adjustment of Eh is not normally required after O_2 removal and freezing but may be checked. This procedure is used to avoid free fines and solution species (not adsorbed) drying down onto the mineral surfaces in the vacuum of the microscope or spectrometer. It is necessary only if the ionic concentration of the solution exceeds 10^{-3} M. Samples can then be analyzed by XRD, scanning electron microscopy (SEM), X-ray photoelectron spectroscopy (XPS), or time-of-flight secondary ion mass spectroscopy (TOF-SIMS) as explained in the next section.

Sampling from Laboratory Tests

The same principles apply to sampling from lab flotation where changes of reagents (collectors and collector combinations, activators, depressants, flocculants) or conditioning (e.g., agitation, aeration) are being tested before possible changes to plant operation. The samples of feed (successive) concentrates, and tails should be deoxygenated, frozen, and delivered to the surface analysis lab in this form. This is normally done only for samples from tests that have shown significant improvement in flotation recovery or grade. The surface and other analysis can then define the parameters that have changed in the improved flotation for information to the plant operation.

ANALYTICAL SEQUENCE

The most direct and cost-effective sequence of analysis to determine the factors likely limiting recovery and/or grade is that suggested in Figure 1. The techniques (and acronyms) in the sequence are explained in more detail in this chapter, but some initial comments may be helpful. More-specialized mineralogical analysis used as described here may directly indicate that there are factors unrecognized in standard mine mineralogy and liberation studies (e.g., amorphous minerals, residual thin surface layers) or that there has been a change in the proportion of fine and ultrafine particles, including clays and silicates, likely to interfere with value mineral surfaces.

Solution assays of the pulp after conditioning are often available in routine site analysis (but they need to be complete for all species, as discussed below). They can be used in freely available software to model potential precipitates and solution species (at thermodynamic equilibrium) that may adsorb on value mineral surfaces, particularly where this solution speciation has changed because of run-of-mine (ROM) or processing changes. This information should be used with some caution because the time from comminution through flotation is not as long as required for steady state of some of the predicted species, and some of the modeled reactions may

have metastable species. It is valuable, however, in correlation with the surface species (precipitates and adsorbed species) interfering with flotation identified from surface analytical techniques. It may indicate the origin of these interferences in process water and pulp solutions.

The relatively simple ethylenediaminetetraacetic acid (EDTA) chemical extraction can be done in most site labs and can also provide insight to changes in ore oxidation (e.g., oxidized zone, longer-term stockpiling) and the presence in solution of metal ion species, particularly Cu, Pb, and Ag, which are likely to induce inadvertent activation of gangue minerals after collector addition.

The use of SEM in different imaging (i.e., secondary electron, backscattered electron) modes with energy dispersive spectroscopy (EDS) analysis is well known, readily accessible, and low cost. In many cases, it can provide direct observation of surface interference by revealing attachment of hydrophilic particles not available from standard QEMSCAN or MLA imaging.

Finally, the more specialized surface analytical techniques of XPS and TOF-SIMS are now used to specifically define the chemical species (including reaction products, adsorbed species, activators, collectors), their spatial and statistical distributions on the same mineral between feed, concentrate, and tail, or between successive leach samples.

A brief introduction follows for each step in the sequence.

Mineralogy

Mineralogy of the flotation feed is normally assessed as part of liberation studies and whenever the ROM changes significantly. The excellent primary tools for mineral structure and liberation analysis, QEMSCAN and MLA, are well known and widely used (Smart et al. 2007). They are essentially based on compositional identification of minerals. They do not, however, separate crystalline from amorphous phases, identify different mineral structures with the same composition (e.g., sphalerite, wurtzite) or different elemental substitution, and are practically limited to >5 μm particles. The problems with mineralogy in low grade and recovery can be in unrecognized fractions of ultrafine (<200 nm) clays and clay aggregates (<2 μm; e.g., kaolin, smectites, illites) and in amorphous minerals (e.g., silica, talc- and chlorite-like fines) that surface-attach more readily than crystalline forms. Hydrophilic clays and amorphous minerals can be attached to value mineral surfaces with direct influence on the hydrophobic/hydrophilic ratio adversely affecting bubble attachment and flotation. High-clay ores are well known to be problematic, often requiring greater collector dosages. The effects of clay aggregates and mineral surface forms in both the pulp and froth phases affecting rheology, viscosity, and flotation, particularly entrainment, are now well known.

Less well recognized is the presence of relatively high concentrations (5−40 wt %) of amorphous minerals, usually hydrated, in oxidized and high-clay ores (e.g., Smart et al. 2014b). These amorphous mineral particles are normally fine (<10 μm) and may attach to hydrated areas of partially reacted surfaces increasing the hydrophilic load. They are not recognized in XRD mineralogical analysis, and they may be interpreted in QEMSCAN or MLA compositional analysis as crystalline minerals although they will behave very differently in processing (e.g., quartz versus hydrated silica).

Amorphous identification and content can be estimated using a combination of quantitative XRD, bulk assay, and QEMSCAN or MLA. Table 1 from a high-clay ore (Smart et al. 2014b) shows an example where the amorphous material is found to be mainly hydrated silica with additional implications for slime coatings. Amorphous calcium sulfate and chlorite-like phases are also common in other examples.

Table 1 Comparison of mineralogy of a high-clay ore feed between Rietveld XRD and QEMSCAN analyses

Minerals	Rietveld XRD, wt %	QEMSCAN, wt %	QEMSCAN Minus Rietveld XRD, %
Quartz	42	57.7	15.7
Kaolinite	18	11.5	–6.5
Smectite	—	4.5	4.5
Albite	20	15.9	–4.1
K-feldspars	—	0.3	0.3
Muscovite	9	5.4	–3.6
Other silicates	—	0.3	0.3
Carbonates	—	0.3	0.3
Ti(Fe) oxides	—	1.1	1.1
Fe(Mn) oxides	—	0.4	0.4
Pyrite	1	0.4	–0.6
Cu(Fe) sulfides	—	0.3	0.3
Ca sulfates	—	0.0	0.0
Phosphates	—	0.0	0.0
Others	—	1.8	—
Amorphous	11	—	–11.0

Adapted from Smart et al. 2014b

The principle is to use quantitative XRD estimation (e.g., Rietveld analysis using TOPAS software (Coelho Software 2016) with a known (e.g., 15 wt %) added corundum (crystalline Al_2O_3 in the same size fraction). This refinement of other crystalline minerals in Bruker-AXS's TOPAS is then calculated relative to the known and defined 15-wt % corundum addition. Whereas the total of all these minerals and corundum is less than 100 wt %, the additional fraction defines the total amorphous content (not detected in the XRD) in the ore. Finally, these fractions are recalculated to 100 wt %, eliminating the corundum to estimate the wt % amorphous content of the ore (i.e., 11 wt % in Table 1). Other more-detailed methods for determining amorphous content from XRD are reviewed in Madsen et al. (2011). This set of crystalline minerals and amorphous material can then be compared with the compositional analysis of the sample by QEMSCAN analysis or MLA to identify the composition of the XRD amorphous fraction. It is important to emphasize that these two techniquues identify minerals only by their composition although the results are often, or usually, taken to imply crystalline structure. In Table 1, the majority of the amorphous content is in the "quartz" fraction of the QEMSCAN analysis and is likely hydrated silica or silicate content. The QEMSCAN analysis also has lower clay content in kaolinite and muscovite than XRD but assigns some smectite content that would normally be clearly seen in XRD. All of these differences have implications for processing of the ore, particularly high-clay ores (e.g., Cruz et al. 2013, 2015a, 2015b; Zhang and Peng 2015; Farrokhpay et al. 2016; Xu et al. 2014).

Mineralogy can now also be probed for single particles using micro-diffraction with a routine spatial resolution of 10−20 μm when using a laboratory X-ray source and 1−2 μm when using a synchrotron radiation X-ray source.

Micro-diffraction enables specific identification of trace phases that would otherwise not be identifiable in bulk diffraction patterns of complex mineral assemblages. Micro-diffraction does not require complex sample preparation. For analysis of the same sample area, it may be carried out on thin sections or, where this is not necessary, particles may simply be attached to adherent with a noncrystalline tape. Unlike bulk diffraction (with internal standard), micro-diffraction cannot be readily used for mineral quantification because of limitations in the area that may be scanned (i.e., counting statistics) and technical issues in quantitative refinement arising from preferential mineral particulate orientation.

Micro-diffraction is particularly useful where high-value elements with significant compositional and structural variation (e.g., U-containing phases [Gerson 2016] and Ni-containing phases [Fan and Gerson 2011]) are the focus of interest in tailings or leach residue samples as a means for process optimization and improved recovery. Whole areas may be subject to micro-diffraction or entire micro-diffraction maps collected. This enables correlation of variation of mineral phases to flotation or leaching recovery. These different mineralogical forms are often missed by techniques such as QEMSCAN and MLA.

Solution Speciation Modeling

Determination of solution speciation (i.e., predicted relative abundance of specific dissolved and precipitated chemical species) is readily accessible from solution assays but is not widely used in mineral processing control despite routine use in environmental studies of adsorption and examination of oxidation states for toxic elements. Speciation simulation programs (e.g., GEOCHEM-EZ [Shaff et al. 2010], PHREEQC [Toran and Grandstaff 2002], MINTEQ [Allison et al. 1990]) are available free to download. The caution in their use is that solution concentrations of all cation and anions, pH, temperature, and particularly Eh or oxidation–reduction potential (often not measured) are required input. Gas partial pressures and the presence of specific solids phases can be specified in the estimates. The programs come with their own databases of equilibrium constants, solubility products, and redox couples, including some collector and complexant species. These databases can often be supplemented or edited as required.

The value of these simulation programs for minerals processing is to take a "snapshot" of the system, assuming equilibrium, so that undersaturated but potentially adsorbing species and precipitating supersaturated solids may be identified. This can be compared with SEM and surface analyses to extend the correlation of indirect and direct information on hydrophobic and hydrophilic species. The assumption of species and precipitates at equilibrium should be treated with caution in rougher flotation because of the relatively short time from comminution to flotation, with some species being in metastable states (although most dissolved and some precipitating species will equilibrate in this time). With longer flotation (e.g., scavengers) or in recycle, the equilibrium can be approached for these metastable species. Where the assay data are available, this calculation is nevertheless worth doing to direct the interpretation of the surface analysis to these potential species.

An example of the value of this correlation of solution modeling and surface analysis can be found in defining correct procedures for copper (I) activation of sulfide flotation, avoiding precipitation of hydrophilic copper hydroxide ($Cu(OH)_2$) discussed below in more detail (Gerson and Jasieniak 2008; Gerson et al. 1999). In this case, the equilibrium states of both dissolved and precipitated species are found in the time of the conditioning.

EDTA Extraction

This technically simple chemical-based analysis dissolves oxidized metal ions (i.e., Cu^{2+}, Fe^{3+}, Zn^{2+}, Ni^{2+}, Pb^{2+}) as EDTA complexes these ions in situ from surface reaction layers, adsorbed colloids, precipitates, and ions to give solution assays that provide a bulk estimate of the extent of oxidation of all minerals. It does not dissolve these ions from the unoxidized mineral surfaces of sulfides or from crystalline silicates and other bulk minerals. Hence, it provides a direct measure of the extent of oxidation (total extraction) and of specific metal ion availability in the sample (pulp, concentrate, tail, and leach). Comparison with chemical information (i.e., species and composition) from specific minerals in the surface-sensitive analyses of the top 1−10 nm can then provide a more complete picture of the hydrophilic species likely to be interacting with the bubbles and potentially interfering with flotation or of gangue-activating ions.

An example of the laboratory method is to make up a 3-wt % solution of EDTA disodium salt adjusted to pH 7.5 with NaOH. Then 95 mL of this solution is vigorously stirred and purged with N_2 for 5 minutes. A slurry sample (5 mL) collected from the plant is added to the EDTA solution with 5 minutes of continuous N_2 conditioning. The slurry is then filtered through a 0.45-μm Millipore filter. The filtrate is analyzed for metal ions by standard methods. The solids are retained to obtain the sample dry weight and specific surface area, enabling calculation of the mass of metal oxidation species per unit mass of solid. Examples of the methodology and its use in this way can be found in Gerson and Jasieniak (2008).

An example of its use in diagnostic leaching of galena and its oxidation products (Greet and Smart 2002) demonstrated that all oxygen-containing galena oxidation products (i.e., sulfate, hydroxide, oxide, and carbonate, but not polysulfide or sulfur) are rapidly solubilized in EDTA. EDTA does not extract lead from unreacted galena. Continued extraction of lead with increasing conditioning time is due to continued galena oxidation, not to the extraction of lead from galena. Argon gas purging minimizes this oxidation, whereas the use of air or N_2 gas purging does not. Using information gathered from these experiments, an improved EDTA extraction technique was developed and compared with other techniques used in the mining industry.

Analytical Scanning Electron Microscopy

The liberation classes by size and by mineral are well described in the automated QEMSCAN and MLA procedures routinely used in control of comminution for optimization of flotation feed, leach preparation, electrostatic and magnetic separation, and separation by gravity (Smart et al. 2007). These techniques are based on recognition of SEM-imaged particles from pixelated back-scattered electron (BSE) images and stereoscopic EDS spectra-identifying minerals by composition in individual particles or locked composites based on their elemental X-ray counts obtained from EDS detectors (four in QEMSCAN; two in MLA). The MLA discriminates many minerals of interest using only BSE information and combines this with information from EDS only

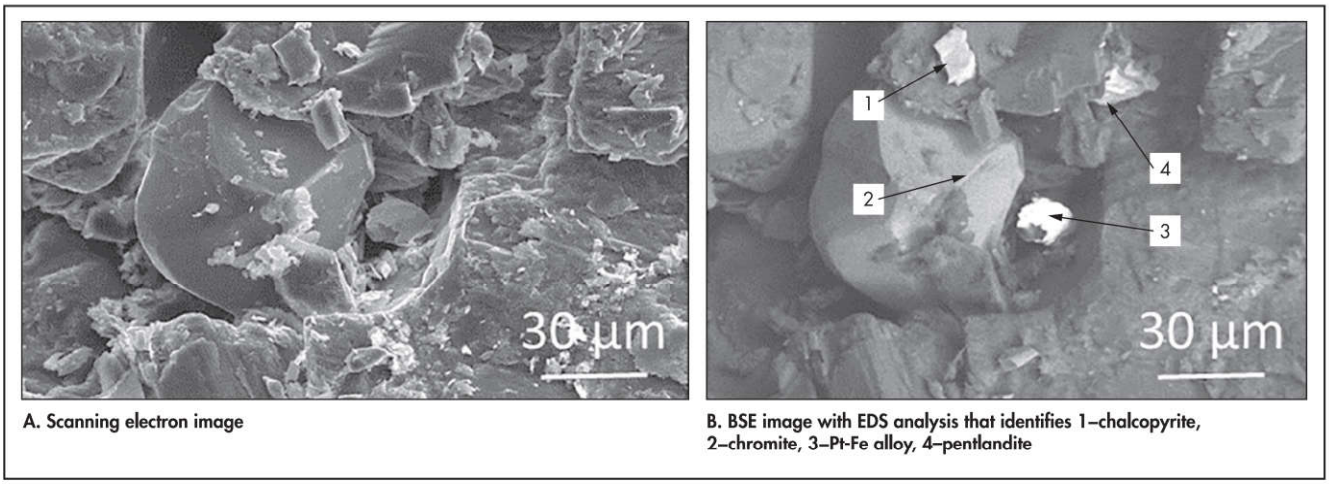

A. Scanning electron image

B. BSE image with EDS analysis that identifies 1–chalcopyrite, 2–chromite, 3–Pt-Fe alloy, 4–pentlandite

Figure 2 Micrographs from a UG2 concentrate for platinum group metals recovery

when needed to discriminate certain specific minerals. These analyses are compared with extensive EDS databases for optimized compositional selection. They can provide quantitative estimates of the percentage of each phase in different particle size fractions and the proportion of each phase in locked composite particles.

In some cases, however, these automated systems may not identify specific mineralogical or surface chemical features interfering with processing. As part of the strategy recommended here, it is always worthwhile to analyze the samples using conventional, low-cost SEM/EDS investigation of individual particles and their surfaces. Identification of different phases and their distribution can be made using SEM/EDS in two imaging modes, illustrated in Figure 2. The scanning electron (SE) image (Figure 2A) primarily reveals pores, cracks, grain edges, and other topographical features. The typical BSE contrast (Figure 2B) is due to compositional variations arising from the atomic number (or density) dependence of the yield of BSEs. More-dense minerals appear in light contrast from higher BSE yield, less dense in darker contrast. In many cases, it is possible to distinguish different phases by the difference in BSE contrast, as in MLA, and thus to map the distribution of each phase. The BSE image does not reveal the structure of pores, cracks, and other topographical features that are more easily seen in the SE image. A "locked," or composite, mineral particle comprising two or more phases can be analyzed by use of the sequence SE imaging, BSE imaging, and EDS analysis.

There can be some forms of incomplete liberation that are not detected in MLA or QEMSCAN analyses that may require more-specific SEM/EDS analysis. Residual locked particles below the size limit of liberation analysis can be responsible for incorrect reporting of gangue or value. For example, at the Kanowna Belle gold mine (Western Australia), a bulk sulfide float for Au in pyrite and arsenopyrite from a predominantly sericite gangue with good liberation assessment was producing good gold recovery but too much sericite in rougher concentrate and consequent smelting issues. SEM BSE images of particles from the rougher concentrate (Figure 3) explained this sericite flotation. The large (>20 µm) sericite (mica) particle in the center foreground of Figure 3 (dark in BSE imaging) has residual pyrite particles <3 µm (light in BSE image) attached to the surface. EDS point analysis confirms this differentiation by recording signals from Fe, S, and O in the partially oxidized pyrite (light region) and from K, Si, and O in the region with dark contrast. These pyrite particles would not be detected in the liberation analysis. With collector addition, they provide multiple hydrophobic points of attachment to bubbles and flotation of large sericite gangue. Outcomes from this study resulted in plant changes to reduce pulp density and increase agitation to decrease recovery of this large sericite, an investment that was recovered in 18 months with ongoing benefit.

Importantly, SEM investigations in these SE, BSE, and EDS modes can provide direct information on fine particles and adsorbed precipitates, at sizes down to 0.5 µm, attached to value mineral surfaces, the first-level identification of interfering particulate forms. Comparison between sample streams will then suggest whether they may be discriminating in recovery or grade. Then they can also be compared with mineralogy, solution speciation, and EDTA extractions for a more complete diagnosis. This may immediately suggest problems with circulating loads of fines (e.g., silicates, talc, micas, clays) or precipitated material (e.g., amorphous $CaSO_4$, iron hydroxides) requiring control.

SEM analyses will not generally identify specific chemical species at the molecular level (e.g., metal-collector precipitates, adsorbed ions). EDS analysis depth is of the order of 1−10 µm and, with imaging limitations (effectively 200−500 nm), it cannot examine the outer molecular surface layers. This requires specific surface analysis techniques of XPS or TOF-SIMS.

Surface Analysis

The introduction and evolution of direct surface analytical techniques in their application to mineral surface chemistry has provided much more comprehensive statistical analysis of ore samples and process stream products. The significance of these techniques is that they provide not only a compositional analysis of the outer molecular surface layers but also information on chemical states (e.g., oxidation, bonding), spatial and statistical distribution of adsorbed species between individual particles, and mineral phases in complex mixtures as a function of depth through the surface layers.

This surface analysis is not carried out in on-site analysis because of cost and specialized operation and interpretation. It

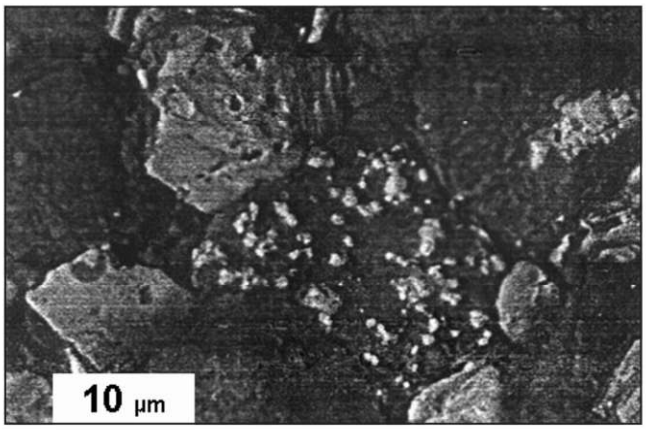

Source: Smart et al. 2014b

Figure 3 BSE image from a rougher concentrate. The large (>20 µm) sericite particle in the center (dark) has pyrite particles <3 µm (light) attached to the surface.

is, however, used in the research and development (R&D) laboratories of some companies, governments (e.g., the Canada Centre for Mineral and Energy Technology), and university minerals processing R&D units. Its main limitations are not in the acquisition of samples or analysis time but in the interpretation of the data. This does require expertise and experience in both the technique and the minerals processing operations to derive the most useful correlations from the large amount of data and implies a dedicated person or group working with company staff. This is normally done as part of the overall application of the strategy working in either project (e.g., industry/government) or in contract mode with the operation.

X-Ray Photoelectron Spectroscopy

In XPS, the sample surface is irradiated with monoenergetic X-rays producing photoelectrons that are analyzed to determine their binding energy. From the binding energy and intensity of a photoelectron peak, the elemental identity, chemical state, and percentage of an element in the top 2−10 nm are determined. These are the first two to five molecular layers in which collector attachment to value minerals may be reduced, obscured, or ineffective in inducing bubble attachment. On gangue minerals, these layers may have inadvertent activated-collector or hydrophobic surfaces. Two-dimensional imaging can now provide species mapping of surface chemistry with a practical spatial resolution of 100 µm, but data collection is relatively slow. In minerals processing, again for practical collection times, it has mostly been used in larger area-average mode (100 µm−1 mm) with limited application to statistical analysis of plant samples. In this mode, it is very useful for defining limitations in chemical processing with collectors, activators, or depressants that are affecting recovery or grade or for defining deposition covering surfaces in flotation or leaching.

XPS has been applied to define many surface oxidation products, including oxidized sulfur species (from sulfide, disulfide, polysulfide, and elemental sulfur to thiosulfate, sulfite, and sulfate) and adsorbed xanthate species on the major base metal sulfide surfaces defining oxidation, collector, activator, and other adsorption mechanisms as well as interfering species, giving more direct insight into the factors affecting recovery and grade. Most of the hydrophobic species, including both reagent and reaction (e.g., polysulfide) products, and hydrophilic species affecting flotation were defined in these studies. The mechanisms and products of in-pulp oxidation and the actions of collectors in partial removal of oxidized species and hydrophobization of the surfaces were studied using XPS combined with other surface analytical methods (Smart et al. 2003a, 2003b, 2007). In particular, the mechanisms of copper sulfate as a flotation activator in sphalerite, in ion exchange with Zn^{2+}, reduction in situ to Cu^{+} with collector attachment, and adjacent oxidation of sulfide to polysulfide-like species were revealed. This has defined the correct plant use of copper sulfate ($CuSO_4$) to optimize sphalerite activation without overdosing, producing hydrophilic $Cu(OH)_2$ precipitation. Inadvertent activation by species such as Pb^{+} and Ag^{+} and actions of depressants, such as cyanide and bisulfite, were also defined in XPS studies. XPS has probably contributed more to understanding of mechanisms of surface chemical actions in flotation than any other surface analytical technique.

In practice now for plant investigations, XPS is normally used in area-averaged mode (100–1,000 particles) to define the ratio of different chemical states between feed, concentrate, and tail or between successive leach samples to define species selectively contributing or interfering with the process. It is differences in the chemical states between the streams that give insight to the selectivity in practice. For instance, sphalerite particles in Cu-activated flotation should be predominantly Cu(I) (complexed with collector) in concentrate, but sphalerite with predominantly Cu(II) as hydrophilic hydroxide is often found in losses to tail (Gerson et al. 1999).

Where grain sizes are larger than 100 µm, XPS may also be used in scanning or imaging mode to define the distribution of specific reagents between mineral phases. An example illustrating the comprehensive information from these techniques is a study of the Inco Bessemer Matte Processing Plant suffering a loss of chalcocite selectivity in flotation separation from Heazlewoodite down the rougher bank (Biesinger et al. 2007). SEM/EDS analyses of the feed, concentrate, and tail samples revealed a decrease in Cu and corresponding increase in Ni recovery through the primary rougher banks with tail samples also containing ≈7 wt % Cu. Suggested mechanisms included inadvertent activation and depression by the dissolution and solution transfer of Cu and Ni ions, lack of collector selectivity, and possible requirement for reaction of the chalcocite surface prior to collector adsorption. The combination of information from SEM/EDS, area-averaged XPS, and XPS imaging clarified the surface chemical mechanisms and control factors in the rougher flotation separation. Chalcocite in the feed to the rougher circuit was unoxidized (i.e., all Cu(I) surface species), whereas the surfaces of the Heazlewoodite appeared to be entirely oxidized to hydroxide species. Chalcocite in the tails from the rougher circuit is more oxidized with evident precipitates corresponding to $Cu(OH)_2$ in both composition and morphology adhering to their surfaces. The primary adsorption of diphenylguanidine (DPG) collector appears to be, correctly, to Cu(I) sites on the unoxidized chalcocite surfaces but is inhibited by the formation or concentration of fine Cu(II) hydroxide precipitates in the later rougher cells. The crystalline morphology of some of the discrete, attached Cu(II) hydroxide precipitates suggested formation in recycle water streams rather than by surface oxidation of the chalcocite through the circuit, although this may not be the only form of Cu(II) hydroxide on chalcocite surfaces in later

cells. Heazlewoodite flotation appeared to be associated with the attachment or locking of fine, unoxidized chalcocite rather than any direct adsorption of DPG; Heazlewoodite fines were also found attached or locked to some chalcocite particles in concentrates contributing to loss of grade. Heazlewoodite was not completely liberated. Heazlewoodite particles in tails had relatively high surface concentrations of attached more-oxidized chalcocite fines, contributing to loss of recovery.

Other examples where XPS has been the technique used to identify interferences can be found in the investigation of galena recovery problems at Mount Isa Mines (Grano et al. 1997) and references therein. The chemical nature of carbonaceous surface layers retained on particles after grinding varies across ore bodies from Mount Isa to Hilton and McArthur River (Saxby and Stephens 1973). In Mount Isa ore, hydrophobic graphitic carbon seen in XPS causes excessive, early flotation of pyrite in the lead/zinc circuit (Grano et al. 1990). In the Hilton concentrator (Grano et al. 1997), XPS revealed the surface carbonaceous material to be less in hydrophobic hydrocarbon and more in oxidized hydrocarbon form, causing slower flotation of pyrite into the concentrate. The XPS signals for graphite and hydrocarbon are distinctly different. XPS surface analysis also found that the presence of significant precipitated calcium sulfate (from lime addition for pH control) on the surface of samples taken from the Hilton concentrator reduces the exposure of metal sulfides in the feed to low levels, restricting the flotation rate of galena when using ethyl xanthate collector.

Time-of-Flight Secondary Ion Mass Spectrometry

In the final stage, if no obvious differences have emerged in the earlier analyses or if confirmation of a suggested limitation is required, it may be necessary to examine the molecular surface chemistry in detail. In flotation, it is the variation of the ratio of hydrophobic/hydrophilic species by particle and as a statistical distribution between different mineral phases across a flotation circuit (e.g., feed, successive concentrates, tails) that may be needed. In leaching, the successive leach samples may require statistical variation of changing surface species. This requires surface analysis of numerous particles with high spatial resolution and chemical speciation, which is not practical with XPS or SEM/EDS. Analyses of a few individual larger particles carries the risk that they may not be representative of the surface chemistry that is causing low value recovery or interfering gangue flotation. It is therefore important to analyze a sufficient number of particles (normally more than 20) of the selected mineral to produce 95% confidence intervals that are discriminatory between the species (e.g., adsorbed, precipitates, collectors) being compared among feed, concentrates, and tails. Alternatively, principal component analysis (PCA) of all particles in the field of analysis provides complete statistics and can be selected by mineral phase.

The technique of choice for this analysis is TOF-SIMS. The parallel development and application of TOF-LIMS, combining laser ionization of small samples with time-of-flight mass spectrometry, by Chryssoulis and colleagues (1992, 1995) at the Advanced Materials Testing and Evaluation Laboratory (AMTEL), reviewed in Smart et al. (2007), and applied particularly to gold flotation interferences, is also acknowledged. The focus here is on TOF-SIMS since this is where statistical analysis has been developed in advanced form.

In TOF-SIMS, a focused (90 nm), pulsed primary beam of heavy ions is directed at the mineral surfaces in fixed, rasterized, or pixelated mode. A fixed beam will analyze a chosen area in the practical range from 90 nm to 1 mm in diameter. A rasterized beam produces lateral images of secondary ion products selected from the total mass spectra collected in the scan. In the pixelated mode, a full mass spectrum is recorded at each pixel (up to 256 × 256 pixels) in a chosen area, giving more than 10^7 data points. Images for any ion can then be selected from this stored data, but, importantly, the data can be statistically analyzed for correlation of surface species within and between mineral phases. For analysis, a very low flux of the heavy ions impacts surface layers so that, in the time of routine measurement, fewer than 5 surface atoms in 1,000 are impacted. The secondary ions, both positive and negative, ejected from these impacts are mass analyzed by charge (m/z) with reversed polarities using their time of flight to the detector. The very high mass resolution m/Δm in the range 7,000−10,000 is able to easily separate almost all closely similar ion masses (e.g., O_2^- from S^-). Secondary elemental ions and molecular fragment ions detached from the first two molecular layers of the surface provide a very detailed set of positive and negative mass fragments from simple ions (e.g., Na^+, OH^-) through to large molecular ions of specific reagents (e.g., isobutyl xanthate $(CH_3)_2CHOCS_2^-$). This data collection generally takes less than 1 hour.

This technique can be applied to rapidly, statistically analyze detailed differences in surface chemistry of selected mineral phases across a flotation circuit or in successive leach samples. Its unique advantages are in being able to analyze the first few molecular layers on a mineral surface for both chemical species (e.g., oxidation products, reagent adsorption, surface layer formation) and spatial distribution (<0.1 μm). The three main forms of information from this technique are selection of mineral particles and their distribution by imaging for specific mineral-selective elements; statistical analysis of hydrophobic and hydrophilic species by comparison of intensities from selected mineral particles between feed, concentrates, and tails; and full statistical analysis by PCA of all species on particular mineral phases. This hydrophobic/hydrophilic ratio varies widely between different particles of the same mineral, and some non-value mineral phases will also have adsorbed hydrophobic collector in some form, contributing to gangue recovery and lower grades (e.g., Trahar 1976; Stowe et al. 1995; Crawford and Ralston 1988; Piantadosi and Smart 2002; Smart et al. 2003a, 2003b, 2007; Boulton et al. 2003; Malysiak et al. 2004; Shackleton et al. 2007).

TOF-SIMS analysis in these modes to identify surface chemical reasons for losses in recovery or selectivity has now been applied to samples from pilot and operating plants, including

- Mount Isa Mines (Australia),
- BHP Billiton's Cannington operations (Australia),
- Ok Tedi Mining Ltd. (Papua New Guinea),
- Teck Cominco Red Dog mine (Alaska, United States),
- Falconbridge (Strathcona, Canada),
- Anglo Platinum (South Africa),
- Mineração Caraiba (Brazil),
- Inco Matte Concentrator (Sudbury, Ontario, Canada),
- Rio Tinto Kennecott Utah Copper (United States),
- LaRonde, Quebec (Agnico Eagle),
- Kittila, Finland (Agnico Eagle),
- Clarabelle mill (Glencore),
- Matagami mine (Glencore),

- Musselwhite mine (Goldcorp),
- Niobec mine (Magris Resources),
- Highland Valley Copper (Teck Resources),
- Thompson (Vale),
- Goldstrike operations (Barrick Gold),
- Kumtor (Centerra Gold),
- Pueblo Viejo, Dominican Republic (Barrick Gold),
- Cerro-Verde, Peru (Freeport–McMoRan),
- Donlin Creek, Alaska (Barrick Gold), and
- Nechalacho, Northwest Territories, Canada (Avalon Resources).

Some details are discussed in the "Case Studies" section later in this chapter.

In some of these proprietary studies and in plant diagnosis follow-up, it has been possible to change plant processes and conditioning to improve flotation. Examples of plant changes have included the following areas:

- **Mineralogy:** ore blending/mixing/storage to control reactivity (pre-oxidation, dissolution), gangue (sulfide, sulfate, talc), and impurities
- **Grinding/liberation:** grind size for liberation but reduced gangue fines; cyclone cuts (narrow); shear, attritioning to control residual and precipitated surface layers
- **Surface oxidation:** control residence time after grind to reduce oxidation products and inadvertent activation; water recycle quality to remove activators or depressant ions
- **Eh/pH:** measure and control for oxidation, collector adsorption, (e.g., galena <200 mV SHE, or standard hydrogen electrode); dithionite, metabisulphite addition; aeration control
- **Surface cleaning:** collector choice; dosages; time after conditioning; cyclone action; high-intensity conditioning; attritioning
- **Activation:** copper ions: monolayer only; critical activation/oxidation time
- **Inadvertent activation:** control of Cu, Pb, Ag ions; oxidation/dissolution reactions; water (recycle)
- **Recycle water:** assay; pH; Eh; depressant ions (e.g., Ca, Mg, sulfate) and fines; settling time; overflow total dissolved solids

In gangue recovery and grade reduction, as in the Kanowna Belle gold mine case study using SEM/EDS, other examples of residual, locked, hydrophobic surface layers causing gangue flotation were found using TOF-SIMS (Smart et al. 2007). However, in these cases, the locked layer was less than 10 nm thick and could not be imaged using SEM/EDS, illustrating the advantage of the TOF-SIMS technique. These examples relate to recovery of gangue pyroxene and chromite in platinum group metals (PGMs) flotation plants. The Merensky (Bushveld Complex, South Africa) ore is processed by bulk PGMs and sulfide mineral flotation, but normally more than 2 wt % of the gangue minerals—principally orthopyroxene with minor chromite, which constitute more than 60 wt % of the ore—report to the concentrate, contributing to subsequent processing costs. Flotation of this gangue can occur through inadvertent copper-collector complexation, but this mechanism does not account for the true flotation of large pyroxene (20−150 µm) particles. Statistical comparison of pyroxene particles between concentrate and tails revealed no significant difference in Cu and collector (isobutyl xanthate or IBX, diethyl dithiophosphate or DTP) TOF-SIMS signals, but surface exposure of talc-like Mg, Si, and O is favored in the concentrate (Figure 4). A statistical comparison of TOF-SIMS analysis of pyroxene particles from concentrate and tails at two different pH values reveals no significant difference in Cu and collector (IBX, DTP) signals, but surface exposure of Mg, Si, and O is favored in the concentrate (Figure 4). Conversely, statistically significant surface species on pyroxene in the tails include the hydrophilic Na, Al, Ca, OH, and SO_3 (oxidation) ions, as might be expected. Collectorless flotation of pyroxene has confirmed this statistical discrimination. The Mg/Si/O association (normally expected to be hydrophilic as adsorbed species) is explained by areas of hydrophobic talc-like residual layers, probably from partial serpentinization of the pyroxene, which can be imaged in TOF-SIMS. Flotation of pyroxene without collector confirmed this statistical discrimination. These ultra-thin (<10 nm) residual layers result from shearing through the relatively soft talc-like material during autogenous grinding. A similar observation of residual talc-like layers has also been found in flotation of chromite in the UG2 Bushveld ores. Plant control through effective depressant action for talc has been extensively tested.

The chapter authors have also observed thin residual layers of soft chalcocite on pyrite surfaces causing excessive misreporting to copper concentrates and requiring resort to

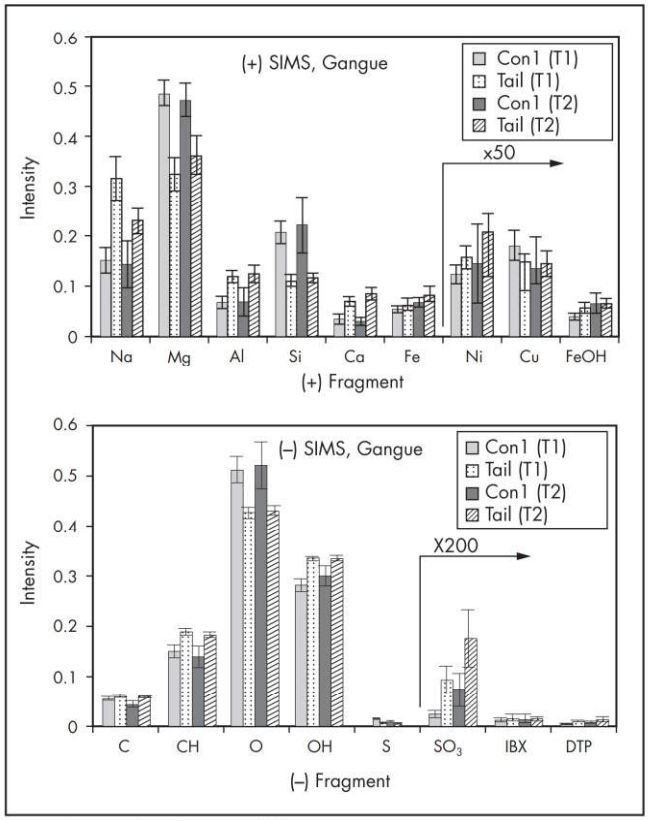

Source: Jasieniak and Smart 2009

Figure 4 Statistical comparison of TOF-SIMS normalized intensities with 95% confidence intervals (error bars) from (+) and (–) mass spectra of pyroxene gangue particles from Merensky Reef ore flotation. Results are shown for flotation concentrates and tailings from two tests (T1, T2) at different pH values.

hydrothermal leaching rather than flotation. This sometimes unrecognized liberation issue, requiring grinding, chemical, flotation, or process changes, can be identified and understood using information from both SEM and TOF-SIMS.

Two other examples illustrate the advantages of the statistical identification of factors discriminating in flotation. A Brunswick Mines plant survey found sphalerite reporting excessively to the copper–lead concentrate. Plant samples were taken in the copper–lead circuit from the rougher feed (RF), rougher bank A concentrate (Con A) and tail (Tail A), and rougher bank F concentrate (Con F) and tail (Tail F). Sphalerite particles were selected using mineral-phase imaging to give reliable statistics. Increased Cu and Pb intensities in the Con A/Tail A pair and Con F relative to sphalerite in the feed (RF) suggested dissolution and adsorption processes in conditioning. TOF-SIMS normalized intensities (Figure 5) displayed as a standard box plot show the range and distribution of both Cu and Pb on the surface of sphalerite grains. The box plot is a standardized way of displaying the distribution of data based on the five-number summary: showing successively minimum, first quartile, median, third quartile, and maximum. The central shaded rectangle spans the first quartile to the third quartile (the interquartile range), which is 1.35σ (standard deviation).

The data suggest that for the Con/Tail pairs in the rougher banks A and F, Cu on the surface of sphalerite grains is discriminating in flotation of the sphalerite in the copper–lead circuit. There is (normally) considerable spread in the surface copper intensities on different particles from plant samples, but the median values with standard deviations discriminate for both sets of Con/Tail samples. Pb, on the other hand, does not show this discrimination in the earlier rougher bank A, but there is large variation in the Pb content on the surface of the sphalerite grains reporting to Tail A. There is discrimination in the down-bank F median values with standard deviations between Con F and Tail F, although intensities are only slightly higher on sphalerite particles from Con F relative to the tail. Cu activation is favored 3−4× over Pb at pH >9 (Sui et al. 1999; Ralston and Healy 1980) so that Pb activation becoming more significant in these later samples suggests decreased Cu concentration in solution. The sphalerite grains that are indeed showing surface Cu in Con F may have been activated much earlier in the stream. A prolonged residence time for sphalerite at pH values ~9 in a Cu-depleted solution would also facilitate the adsorption of $PbOH^+$, enhancing the flotation of grains difficult to recover.

The most recent advance in the statistical analysis of TOF-SIMS data is the use of multivariate PCA, which improves image contrast, mineral phase recognition, and separation of topographic from chemical effects, and it identifies related surface species on particular mineral surfaces. PCA can identify statistical relationships between secondary ions from species that contribute to variation in surface chemistry between minerals and between flotation streams (i.e., feed, concentrates, and tail). This form of analysis can be applied to an entire mapped area of TOF-SIMS data without the need to manually define regions of interest. As each set of correlated components is identified, the correlated data are removed from further analysis to enable further correlations to be defined. Each set of correlations is termed a *principal component* (PC) while the degree of correlation of each species within a given PC is termed the *factor loading* (in both positive and negative sets in the PC). The factor loading is not a measure of amount or intensity of that species but of its correlation with other

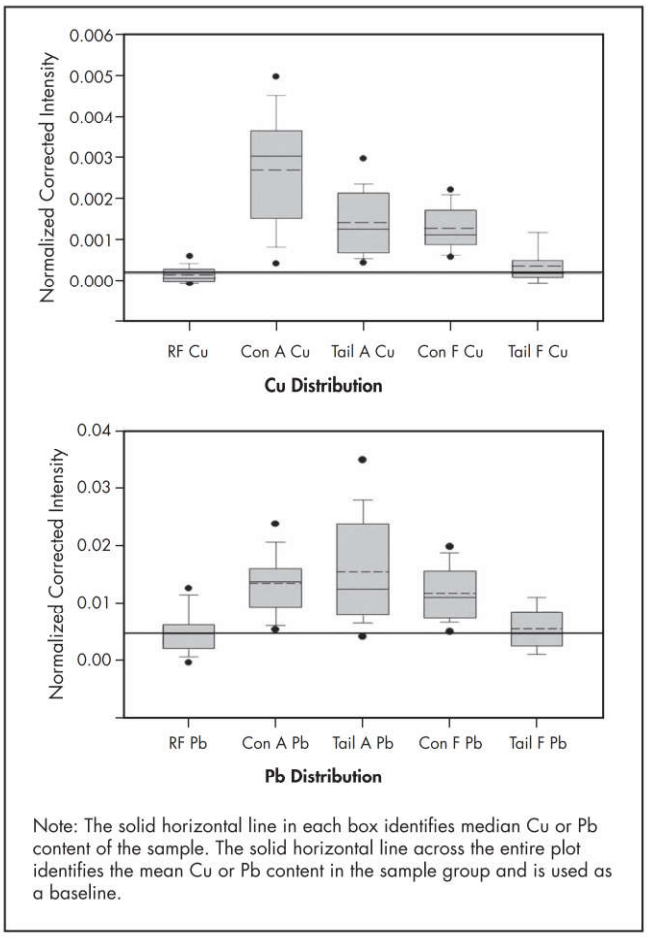

Note: The solid horizontal line in each box identifies median Cu or Pb content of the sample. The solid horizontal line across the entire plot identifies the mean Cu or Pb content in the sample group and is used as a baseline.

Source: Smart et al. 2014a

Figure 5 Vertical box plots for TOF-SIMS analyses of sphalerite surfaces from Con and Tail samples at Brunswick Mines

species in that PC. Many of these PCs immediately identify specific minerals with their associated, correlated surface species. In practice, the first principal component, PC 1, is found to be associated with topographic effects (like a SEM image) and does not hold any chemical information. This surface chemical information appears, after removal of the topography, in PC 2 onward. This analysis can be processed in much shorter time (<1 hour) compared with other techniques.

An example from PCA applied to TOF-SIMS data from a Kennecott Utah Copper (KUC) study to provide chemical diagnosis illustrates the value of the method. This study was also the first to use the full strategy of mineralogy, EDTA extraction, solution speciation modeling, SEM/EDS, and TOF-SIMS. The full set of data, combining mineralogy, liberation, solution speciation, microscopy (SEM), surface analysis, and flotation testing, can be found in Gerson et al. (2012).

The initial flotation stage in the KUC concentrator flotation circuit is the bulk recovery (maximized) of copper and molybdenum sulfides, which are then separated via subsequent flotation steps. The Bingham Canyon porphyry copper deposit, the source of the ore, is geologically complex but can be simplified into limestone skarn (LSN) ore, containing economic concentrations of Cu sulfide minerals, and monzonite (MZ) ore, containing economic concentrations of both Mo and Cu sulfide minerals. It had been proposed, as a result of

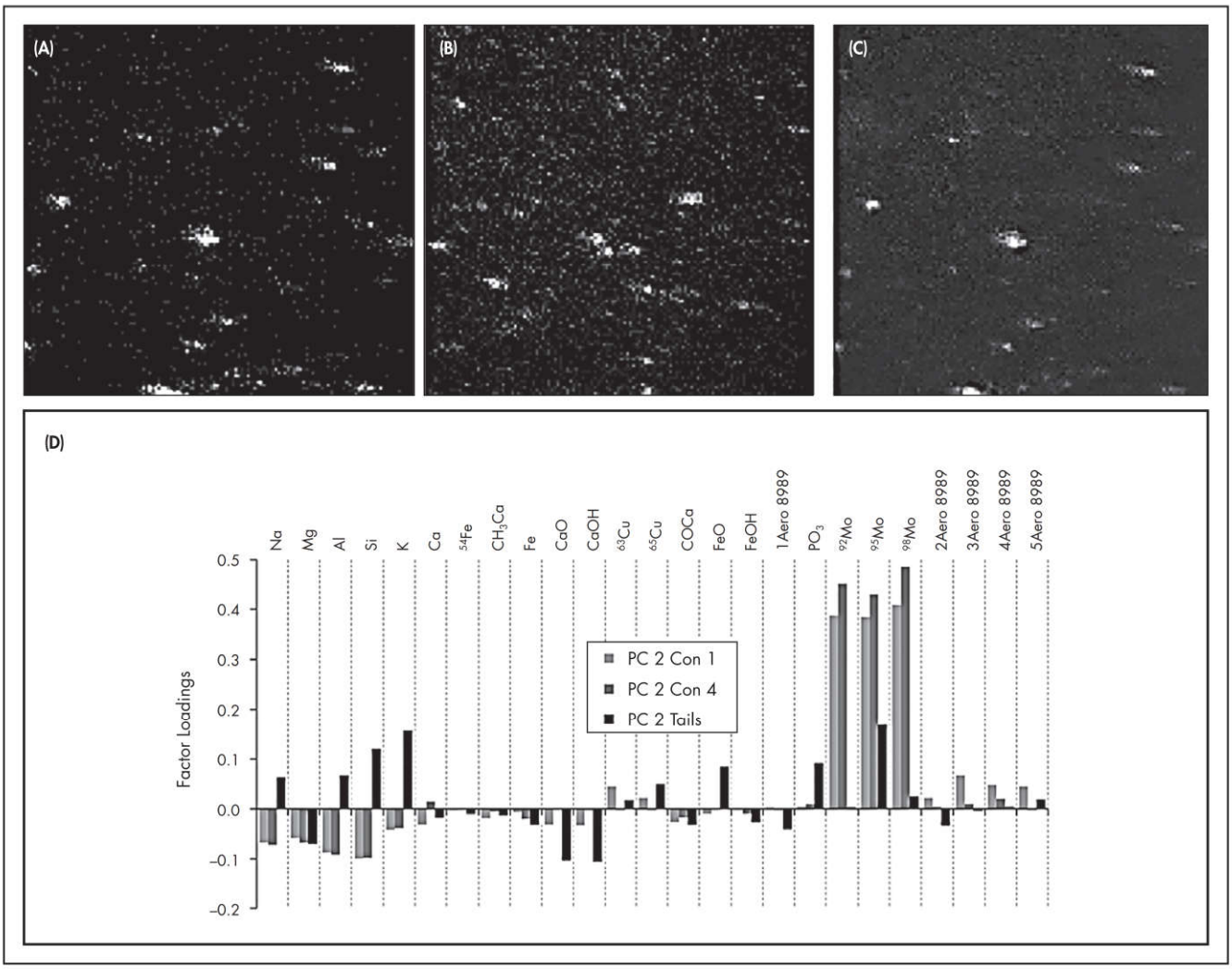

Source: Smart et al. 2014a

Figure 6 500 × 500 µm images of MZ Con 1: (A) TOF-SIMS ^{98}Mo data, (B) TOF-SIMS ^{63}Cu data, and (C) PC 2 showing areas of positive factor loadings as pale. It is clear that there is a high degree of correspondence between PC 2 and ^{98}Mo. (D) PC 2 factor loadings for MZ float Cons 1 and 4 and tails.

plant-based flotation observations, that that blending of these two ore types leads to "poisoning" of the flotation response (Triffett et al. 2008; Triffett and Bradshaw 2008). Laboratory flotation demonstrated that chalcopyrite and bornite recovery was near pro rata in the blend, but molybdenite recovery was substantially adversely affected (Gerson et al. 2012). PCA TOF-SIMS on the laboratory concentrates and tails from MZ, LSN, and blended (70:30, respectively) feeds was used to explain these differences in behavior.

PCA factor loadings from the MZ float experiments found a very strong correlation of all three Mo isotopes in PC 2 from Con 1 specifically identifying molybdenite surfaces (Figure 6D). An indication of the significance of a species identified in a given PC may be obtained by examining maps of the PC as compared to images of the actual mass fragment distribution (e.g., Figures 6A, 6B, and 6C). The lack of significant correlation to other species, except a minor correlation to hydrophobic Cu-collector fragments (dicresyl dithiophosphate), shows very clean molybdenite surfaces. In contrast, significant correlation of Cu isotopes with Fe, suggesting identification of bornite and chalcopyrite, is only obtained in PC 4 where this is correlated to both hydrophobic collector fragments and hydrophilic FeO, FeOH fragments, K, and Mg species. MZ Con 4 still displayed a very strong correlation of the Mo isotopes in PC 2 (Figure 6D). In this later concentrate, no PCs identifying strong factor loadings for Cu and Fe were found, suggesting that the surfaces of the copper-containing minerals were largely obscured by oxidation and/or attached particles. For the MZ tail, no Mo isotopes were found in PC 2 (Figure 6D) and were only weakly selected in PC 4, but no Cu and Fe association was observed. These statistical correlations show that, while the surfaces of molybdenite were relatively clean in Cons 1 and 4, the surfaces of the Cu-containing minerals carried a much higher hydrophilic loading and were substantially obscured.

A similar trend was found for the Cu-containing components of the LSN ore. An increasing surface loading of Ca-containing and other hydrophilic components was

observed as demonstrated in Table 2. For the blended ore, PCA TOF-SIMS from copper-containing minerals in concentrates and tails was similar to that for the MZ and LSN ores with a relatively high hydrophilic species surface loading that increased through the flotation process (i.e., from Con 1 to Con 4 to tails). However, the PCA TOF-SIMS analysis for the blended ore after Con 1 did not select Mo in any PC for either Con 4 or the tails, in contrast to the MZ ore analyses, showing either very low concentrations or high surface coverage of the molybdenite.

Table 2 Absolute factor loadings for PC 4 MZ flotation experiment

Species	Con 1	Con 4	Tails
^{63}Cu	0.37	0.17	0.07
Fe	0.20	0.04	0.01
Ca	0.10	0.13	0.28
CH_3Ca	0.01	0.07	0.13
CaO	0.06	0.07	0.21
CaOH	0.01	0.14	0.21

Source: Smart et al. 2014a

These PCA TOF-SIMS analyses show that the surfaces of the copper minerals within both the MZ and LSN ores already carried significant Ca-containing and other hydrophilic components so that, on blending, their hydrophobic/hydrophilic ratio after collector addition did not change significantly and their flotation response remained acceptable. However, the surfaces of the molybdenite component of the MZ ore before blending were largely clean. On blending, partial transfer of the Ca-containing and other hydrophilic components as precipitates, colloidal, and adsorbed ions in the LSN ore took place on the MZ molybdenite particle surfaces, resulting in apparent poisoning of the flotation response of this component. Unless other factors apply (e.g., stockpiling, throughput), there is no flotation benefit from blending these ore types. KUC no longer blends these ores.

Hydrophobic/Hydrophilic Indices

The TOF-SIMS statistical analysis has been applied to the effects of calcium ion depression on a galena flotation (Piantadosi et al. 2000) using collector adsorption of both IBX and DBPhos. This analysis illustrates hydrophobic/hydrophilic ratio differences between minerals in concentrates versus tails. Linear regression and mean analyses of surface species on galena particles in the first concentrate and tail (sets of 26 particles) were used to estimate hydrophobic (e.g., $DBPhos^-/SO_3^-$) and hydrophilic (e.g., Ca/Pb, Al/Pb, PbOH/Pb, SO_3^-/S_2^-) indices. The results correlated closely with the flotation response. Hydrophilic species indices such as calcium (≈2×), but also aluminum and metal hydroxides, were statistically greater on tail than on concentrate particle surfaces. This method suggested that it was possible to quantitatively assess conditioning of sulfide surfaces for optimum selectivity although this full ratio determination is not normally required in plant sample determination of interfering factors.

A second statistical study (Piantadosi and Smart 2002) of the effect of iron hydroxide oxidation products and collector, IBX, on galena and pyrite flotation separation at pH 9 confirmed a clear separation of IBX normalized intensities with galena in concentrate 5 ± 1.5× greater than those in either feed or tail. A hydrophobicity/hydrophilicity index, based on a ratio of signals from the hydrophobic collector (IBX) to ions from hydrophilic oxy-sulfur products (SO_3) and iron hydroxide (FeOH), gave a value for the concentrate of 45 ± 14 compared with 7 ± 2 for the tail. A similar differentiation was found using DBPhos collector. These hydrophobic/hydrophilic indices systematically decrease across the flotation sequence between concentrates 1, 2, 3, and tail (Smart et al. 2003b) and can be used to diagnose parts of the circuit in which this ratio is not effective for bubble–particle attachment, therefore requiring changes to conditioning procedures.

EXAMPLES OF INTERFERENCES WITH SELECTIVITY

Common Surface Layers

This section summarizes and provides comments on surface layers and species often found in the chapter authors' analyses of plant samples, which include the following:

- Iron hydroxides in colloidal and floc form (2 nm–5 μm), resulting from oxidation of iron sulfides and precipitation above pH 3. They are generally seen on all mineral surfaces and are not discriminatory for value mineral flotation between concentrate and tail. At high surface loads, often caused by high concentrations in recycle water, they can reduce flotation kinetics of value minerals, causing lower grades in later cell recoveries.
- Adsorbed calcium ions and amorphous hydrated calcium sulfate (not crystalline gypsum) precipitates, both strongly hydrophilic species, often significantly reduce recovery and grade. These species can result from dissolution of soluble calcium minerals, as in the KUC case study, or from lime addition to control pH and inadequate removal in thickeners and recycle water. In some plants, the authors have seen up to 70% coverage of value mineral surfaces by these species, severely reducing availability for attachment of collector. Replacing lime with soda ash for control up to pH 9 is an option for improved recovery, but relative cost factors need to be evaluated and this is not often carried out.
- Generally reduced exposure of value mineral surfaces due to extensive attachment of fine silicate minerals, clays, and micas from comminution of the ore-reducing collector attachment and flotation or leaching kinetics. This is often seen where prior oxidation or reaction/dissolution of the ore has occurred in ROM, storage, or excessive aeration before flotation and the surfaces of the value minerals are already sufficiently hydrophilic that these additional hydrophilic fines readily attach. This may be indicated in EDTA extraction and requires checking back to the point of oxidation increase. This is exacerbated at higher pulp densities and can often be reduced by lowering pulp density and/or increasing agitation as in the Kanowna Belle gold mine case.
- Inadvertent activation of a value mineral in the wrong part of the circuit, particularly sphalerite in lead circuits, or of gangue minerals generally. This is usually caused by dissolution of other minerals providing the activating ions to which collectors will attach, including Cu(II), Pb(II), and Ag(I). This may again be due to ROM, storage, or excessive aeration before flotation. The BHP Billiton case study later in the chapter illustrates this problem. Where excessive gangue mineral flotation occurs with

collector identified on these surfaces, this may be due to the combination of the activating ion dissolution and collector overdosing. Formation of ion-collector complexes in solution, rather than on the value surfaces, can result in indiscriminate attachment to all mineral surfaces, severely reducing grade.
- Other factors discussed previously, including residual layers and hydrophobic mineral attachment (particularly talc) activating surface layers on gangue minerals, can be identified in this strategy.

EXAMPLES OF INCORRECT CONDITIONING

Collector Attachment, Inadequate Coverage, and Comparisons Between Collectors

The attachment of specific collectors to specific minerals can be imaged in TOF-SIMS, and their effectiveness in flotation selectivity can be assessed in statistical comparisons of their signals between concentrate and tail samples. Where flotation kinetics are too slow, causing low selectivity in later cells, the coverage of value mineral surfaces by collector can be imaged to assess whether this is due to inadequate coverage and consequent low hydrophobic/hydrophilic ratios. Early studies by Brinen and co-workers at Cytec (Brinen and Reich 1992; Brinen et al. 1993) and by Chryssoulis and his AMTEL group (Stowe et al. 1995; Chryssoulis et al. 1995) confirmed that this technique can identify parent and fragment ions from collectors and map their distribution on single-mineral grains. Comparisons between the effectiveness of different collectors separately or in mixtures can now be assessed in the statistical mode. An example from a BHP Billiton Cannington plant survey (described in more detail in the "Case Studies" section) illustrates this discrimination. A relatively high recovery of sphalerite to the lead circuit cleaners represented losses for the zinc circuit. The flotation used a combination of ethyl xanthate (EX) and DBPhos collectors. Following a formal plant survey analysis, 26 particles of sphalerite from the lead cleaner concentrate and tails were investigated by imaging for Zn-containing secondary ions. In the statistical analysis, the separation of intensities from specific species at more than the 95% confidence interval indicates that these species discriminate between the two streams. As Figure 7 shows, because of the wide spread of intensities, there is no separation at more than the 95% confidence interval between sphalerite particles from cleaner concentrate and tail for either collector. The mean value for the collector DBPhos molecular ion on concentrate particles is, however, 50% greater than in the tail, but EX mean values are not very different between cleaner concentrate and tail. The EX intensities still indicate that this collector would have contributed to sphalerite being recovered in hydrophobic complexes with Cu, Ag, and Pb into the lead roughers and scavengers before the cleaners (as explained later in the case study). The results suggest that the EX does not cause as much sphalerite loss as DBPhos in the lead cleaner separation. This result led to a reexamination of the collector mixture used in the lead cleaner circuit.

Effectiveness of Conditioning Reagents

The detail from surface analysis can suggest changes to conditioning, residence time, and Cu deactivation reagents. For instance, Zn activation control in an industrial Cu flotation circuit treating a complex Cu-Pb-Zn-Au-Ag sulfide ore at the LaRonde Division of Agnico Eagle Mines Limited (Quebec, Canada) was investigated through COREM (Olsen et al. 2012). The action mechanisms of zinc sulfate ($ZnSO_4$), triethylenetetramine (TETA), and sodium bisulfite ($NaHSO_3$) used as depressants to limit ZnS activation were examined. A combined TOF-SIMS/XPS examination of sphalerite surfaces in copper plant samples with Cu^{2+} addition was performed to evaluate the response to the three depressants. Although copper transfer occurred under all test conditions, both the $ZnSO_4$ and TETA test samples indicated that Cu was partially inhibited from attaching to the surface of the sphalerite grains. The operational mechanisms, however, were probably different: the former likely related to the development of oxidative species on sphalerite grains, and the latter to the chelating capacity of TETA (Tukel et al. 2010). Sphalerite surfaces in both the $ZnSO_4$ and $NaHSO_3$ tests reported the highest proportion of species, indicative of oxidation such as $Zn(OH)_2$ and SO_3. It is possible that greater development of sulfoxyl and hydroxide species on the surface of the sphalerite, as identified by TOF-SIMS, may inhibit collector attachment, produce hydrophilic surfaces, and, in combination, result in reduced sphalerite flotation (Chandra and Gerson 2006). In another example, carboxymethyl cellulose (CMC), commonly used as a depressant for talc-like minerals, was studied in the TOF-SIMS imaging mode using CMC fragments by Parolis et al. (2007). These authors showed that CMC coverage of the talc particles was homogeneous after initial adsorption, but subsequent desorption in distilled water partially restored flotability and this change could be related to an inhomogeneous CMC distribution on the talc surface. Additional exposure to Ca^{2+} ions gave homogeneous CMC redistribution and depressant action.

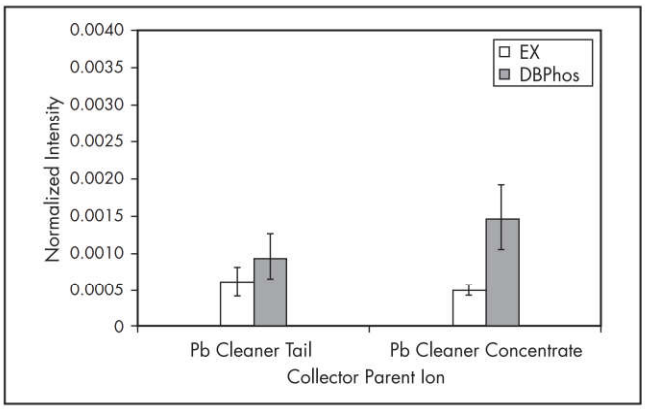

Adapted from Smart et al. 2003b

Figure 7 Statistical comparison of TOF-SIMS normalized intensities for collector ions EX and DBPhos on sphalerite particles from a lead cleaner concentrate and tail (bars = 95% confidence intervals)

Incorrect Cu Activation—Overdosing

There is considerable misunderstanding of activation mechanisms and their control in flotation, resulting in incorrect conditioning in some plants. A short explanation of the mechanism (Chandra and Gerson 2006) may be helpful to consider in plant control.

Both sphalerite and pyrite can be activated by ions such as Cu^{2+}, Fe^{2+}, Ag^{+}, and Pb^{2+} in solution; however, it is only $CuSO_4$ that is normally added in flotation practice. Sphalerite will not normally adsorb thiol collectors and float without copper activation. Copper addition is also used to assist bulk

sulfide and pyrite/pyrrhotite flotation for associated gold or PGM recovery. The other ions resulting from reaction and dissolution are normally considered contaminants, which can cause inadvertent activation and loss of selectivity, particularly where sphalerite flotation and pyrite depression are required. XPS studies have shown that copper activation of sphalerite proceeds with a 1:1 exchange of Cu^{2+} with Zn^{2+} from the first few atomic layers of the sphalerite surface, after which a surface Cu^{+}-S^{-} species is formed. XPS can clearly separate Cu(II) and Cu(I) species to allow assessment of correct conditioning in formation of the Cu(I) species. This surface Cu(I)-S(−I) species formed is hydrophobic and can induce some collectorless flotation, but the addition of collector to form the stable Cu(I)-collector (e.g., xanthate X(−I)) complex induces stronger hydrophobicity. With time after Cu(II) addition, it will continue substituting with Zn and slowly migrate into the bulk, potentially reducing the surface concentration for finite dose. Under conditions of long activation time between copper activator and collector addition, concentrations of Cu(I)-X(−I) formed on the surface may be relatively low, which may affect flotation. Hence, both the total amount of Cu(II) and time after addition before collector addition are important parameters for correct conditioning.

Pyrite activation, however, follows a single fast step involving Cu(II) adsorption to the surface without any exchange with iron in the pyrite lattice. Unlike sphalerite, pyrite adsorbs thiol collectors and floats well even without copper activation because of the activating nature of Fe^{2+} on pyrite surfaces, where Fe-X_2 structures can form along with neutral dixanthogen X_2. This flotation is stronger in low-pH conditions as the surface Fe^{2+} sites oxidize to form iron hydroxide species at higher pH, which retards collector adsorption. This gives improved selectivity for sphalerite/pyrite separation but generally lower kinetics for bulk sulfide and pyrite/sphalerite recovery.

These mechanisms dictate that copper addition should ideally be just sufficient to form the adsorbed outer surface monolayer on the mineral to be floated with collector addition as soon as possible after activation. This will maximize the hydrophobicity of these surfaces. Overdosing copper, sometimes done in PGM flotation to control froth structure, works against the selectivity of these mechanisms. At pH above about 6, hydrophilic colloidal $Cu(OH)_2$ will precipitate onto mineral surfaces and a thick obscuring layer of $Cu(OH)_2$ may form if the conditioning copper concentration is relatively high. $Cu(OH)_2$ precipitates nonselectively and has the potential to cause flotation of unwanted minerals or gangue, through slow subsequent reduction of Cu(II) and reaction with xanthate to form Cu(I)-X(−I) and dixanthogen X_2, both hydrophobic species, particularly if the collector is also overdosed. The $Cu(OH)_2$ layer also obscures the Cu(I)-S(−I) layer on sphalerite, further reducing surface hydrophobicity.

Overdosing collector is equally disadvantageous to selectivity. At excess dosages, hydrophobic dixanthogen forms in solution as nano-colloidal oily droplets and tends to adsorb nonselectively, causing unwanted flotation of non-value minerals, especially gangue. Xanthate may also react with Cu^{2+} in the conditioning solution, causing precipitation of Cu-xanthate in the solution and, again, nonspecific adsorption. This limits the amount of xanthate available for floating the desired mineral, thus increasing reagent consumption. Sequential addition of copper and xanthate is consequently preferred over simultaneous additions of these reagents.

The presence of a high lattice iron concentration in sphalerite, which occurs in some deposits or is a variable in flotation recovery, is an intermediate case. It has caused increased adsorbed copper and subsequently higher xanthate adsorption but lower adsorbed copper and xanthate adsorption in other conditions. The reason for this discrepancy lies in the higher reactivity imparted to sphalerite by high iron content. Sphalerite containing high iron oxidizes much faster than low-iron sphalerite and at high pH is likely to be covered by hydroxides possibly at iron sites, which may be located near steps or defects. Control of surface pre-oxidation (e.g., storage, processing time, and aeration conditions) and pH is therefore critical for optimized flotation of high-iron sphalerite.

An example of the combined use of EDTA extraction, solution speciation, XPS, and TOF-SIMS has also illustrated the importance of pre-oxidation in control of copper activation of pentlandite, and monoclinic and hexagonal pyrrhotite in a PGM recovery circuit (Gerson and Jasieniak 2008). It has been established in a laboratory simulation that the addition of $CuSO_4$ in conjunction with xanthate collector increases the flotation rate of pentlandite as compared to the addition of collector alone. However, it remained unclear whether the addition of $CuSO_4$ has a similar effect within mineral processing circuits and whether this also applied to the alternative forms of pyrrhotite. Activation experiments were carried out at pH 9 using a total solution content of copper ions equivalent to one monolayer. Copper loss from solution was extremely rapid in all cases with less than 10% remaining after 10 seconds. Immediately after collector addition, EDTA extraction, solution analysis, and XPS clearly demonstrated that copper activation on all three minerals was via direct surface adsorption and not an ion exchange process, as is the case for sphalerite, and that most copper on the surfaces is in the form of Cu(I).

Testing increased conditioning time prior to copper activation, and TOF-SIMS analyses of the mineral surfaces subsequent to copper activation demonstrated increased surface oxidation. Regardless of the length of pre-activation oxidation time, only Fe(III) (no Fe(II)-S) was observed by XPS analysis on all three minerals, indicating a highly oxidized surface layer dominated by Fe-O-OH species. The presence of Cu(II) on the mineral surfaces is indicative of the formation of Cu(II)-containing precipitates and indicates non-mineral-specific activation, resulting in increased recovery but lower grade. Mineral-specific copper adsorption, as evidenced by the presence of Cu(I), is required to improve both grade and recovery. Prolonged oxidation prior to copper activation causes a reduction in the Cu(I)-to-Cu(II) ratio on the mineral surfaces as compared to either fresh surfaces or surfaces oxidized for one minute only. This strongly indicates that the copper activation process is less effective on highly oxidized surfaces. However, there is a significant decrease in surface oxidation with time on comparison of samples exposed to copper solution rather than water. This suggests that copper activation stabilizes the surface and reduces the rate of oxidation, but this oxidation still requires control for maximum recovery and grade.

Other examples of combined information from solution modeling, EDTA extraction, and surface analysis (XPS) include the flotation study on Cu and Pb speciation as a function of contrasting Eh and pH conditions during grinding (Peng et al. 2012). In the flotation of copper ores, several processing plants reported that copper recovery is affected by the proportion and reactivity of pyrite in the ore with the effect becoming more intense when the feed particles are finer as a result of

regrinding. Flotation tests showed that chalcopyrite flotation rate, recovery, and grade, as well as the pulp oxidation potential decreased with increasing pyrite content although pyrite recovery increased. Surface analysis (XPS, TOF-SIMS, and EDTA) revealed that inadvertent copper activation of pyrite increased with increasing pyrite content, facilitating pyrite recovery (Owusu et al. 2014). Decrease in chalcopyrite recovery was also attributed to increased surface oxidation in association with higher pyrite content or finer grind, both factors reducing recovery and grade.

CASE STUDIES

Base Metal Copper, Lead, and Zinc Flotation

This case study illustrates the sequence of TOF-SIMS analysis normally used for plant samples where the mineralogy, EDTA, solution speciation, and SEM/EDS have not given a clear indication of controlling factors. The operating BHP Billiton Cannington plant in Australia was floating chalcopyrite, galena, and sphalerite in sequence. Sphalerite being recovered to the lead circuit cleaners represented losses for the subsequent zinc circuit. No $CuSO_4$ had been added in the circuit to this point.

Samples were collected from lead cleaner concentrate and tail using the sampling procedure described previously. After initial scans for all species, imaging the spatial distribution of the main surface chemical species is usually the first step in TOF-SIMS diagnosis of surface chemical species controlling recovery and grade. This step is fast and provides the basis for focusing on species that appear to be different between concentrate and tail for the specific mineral phase. TOF-SIMS images of the particles in total ion yield mode as in Figure 8A are similar to those from SEM imaging. Scanning for specific signals (e.g., Pb, Zn, Cu, Fe, Fe/Cu), can then be used to identify the particles of a specific mineral phase (e.g., galena, sphalerite, covellite, pyrite, chalcopyrite) for specific analysis. The region of interest (ROI) facility in the software allows definition of selected particles corresponding to a specific mineral phase with the boundary for analysis set at a fixed position inside the contrast edge. When sufficient particles of the mineral phase have been identified for reliable statistics, a mass spectrum from each particle is recorded and stored. The statistical analysis then determines a mean value for each atomic and molecular species with 95% confidence intervals for each signal.

Sphalerite particles in each sample were identified from the total ion image (Figure 8A) by imaging for Zn as illustrated in Figure 8C. Then other species associated with Zn likely to be discriminating between Con and Tail—in this case Cu, Pb, Ag (identified in these initial scans), and collectors EX and DBPhos—can be extracted from the images, as in Figures 8D, 8B, and 8E, respectively. The spatial distributions in the image analysis show that sphalerite reporting to the cleaner concentrate has adsorbed Cu, Ag, and Pb ions. These ions complex strongly with collectors to produce hydrophobic surface species, inadvertently activating the sphalerite for bubble attachment.

To confirm these discriminating factors causing sphalerite flotation, a statistically valid selection of sphalerite particles from the lead cleaner concentrate and tails was investigated. This statistical comparison is illustrated in Figure 9 where 26 sphalerite particles were selected from plant samples of concentrate and tail (discussed earlier in the "Collector Attachment" section) and images like Figure 8. The TOF-SIMS spectra from each bounded sphalerite particle was collected for the statistical comparisons. The separation of intensities from specific species at a 95% confidence interval indicates that adsorbed Cu, Ag, and Pb positive ions discriminate between sphalerite particles in the cleaner concentrate and those in the tail although these species are present on all sphalerite particles. The negative ions used to discriminate species in the concentrate included C, CH, and collector fragments of DBPhos and EX. These signals all represent hydrophobic species associated with collector adsorption. The hydrophilic surface species that discriminate sphalerite particles into the cleaner tail are positive ions of Mg, Ca, Al, and Si, and negative ions of O, all of which represent aluminosilicate gangue species as fine particles adsorbed to the sphalerite surfaces, decreasing the hydrophobic/hydrophilic ratio on these surfaces. Notice, however, that there are still significant intensities of these species on sphalerite that have reported to the concentrate, confirming the heterogeneity of mineral surfaces in real pulps and the importance of the hydrophobic/hydrophilic ratio in bubble–particle attachment. This "knife-edged" selection of particles reporting to concentrate versus tails is the reality of the flotation process and the reason for surface chemical control.

As noted earlier, the results suggested that the EX does not discriminate as clearly as DBPhos in sphalerite reporting to the lead cleaner concentrate. These combined results caused a reexamination of the collector mixture used in the lead cleaner circuit and of the residence time for conditioning, during which oxidation, dissolution, and adsorption of these activating ions occurred.

Another example of results from samples supplied by the client from rougher and rougher-scavenger flotation is shown in Figure 10. Poor flotation kinetics were exhibited by fine sphalerite (−10 μm) copper-activated down the rougher-scavenger banks. The study aimed to determine whether the poor flotation response by fine sphalerite was due to differences in mineral surface chemistry rather than hydrodynamic collision frequency factors alone. The process characteristics included pH 10.5 adjusted with lime, collector addition of IBX, and copper sulfate activation. Sphalerite particles in the −10 μm size range were selected using the ROI methodology described previously so that the surface chemistry of this mineral phase was examined selectively. The bars in Figure 10 show the median value of each positive and negative ion signal with the 95% confidence intervals indicated by the smaller intervals at the top of each bar. Comparison between the rougher concentrate, scavenger concentrate, and scavenger tail eliminates all species for which confidence intervals overlap as not statistically significantly different (at least to the first level of statistical analysis). It is clear that other signals are statistically different with diverse magnitudes in this comparison. In the selected positive ion species, discrimination into the concentrate streams is indicated for Zn, Cu, and Na with discrimination into the tail for increasing Fe, K, Si, Al, and, particularly, Mg. Low surface concentrations of Ca appear to favor the rougher concentrate but are apparently depressed into the scavenger concentrate and tail. In negative ion SIMS, the concentrates are statistically favored by high exposure of S, CH, and by low surface exposure of F, OH, and O. More detailed examination of the collector IBX signal shows close correlation with the Cu signals. But the oxy-sulfur SO_3 signals are not statistically different between the three streams.

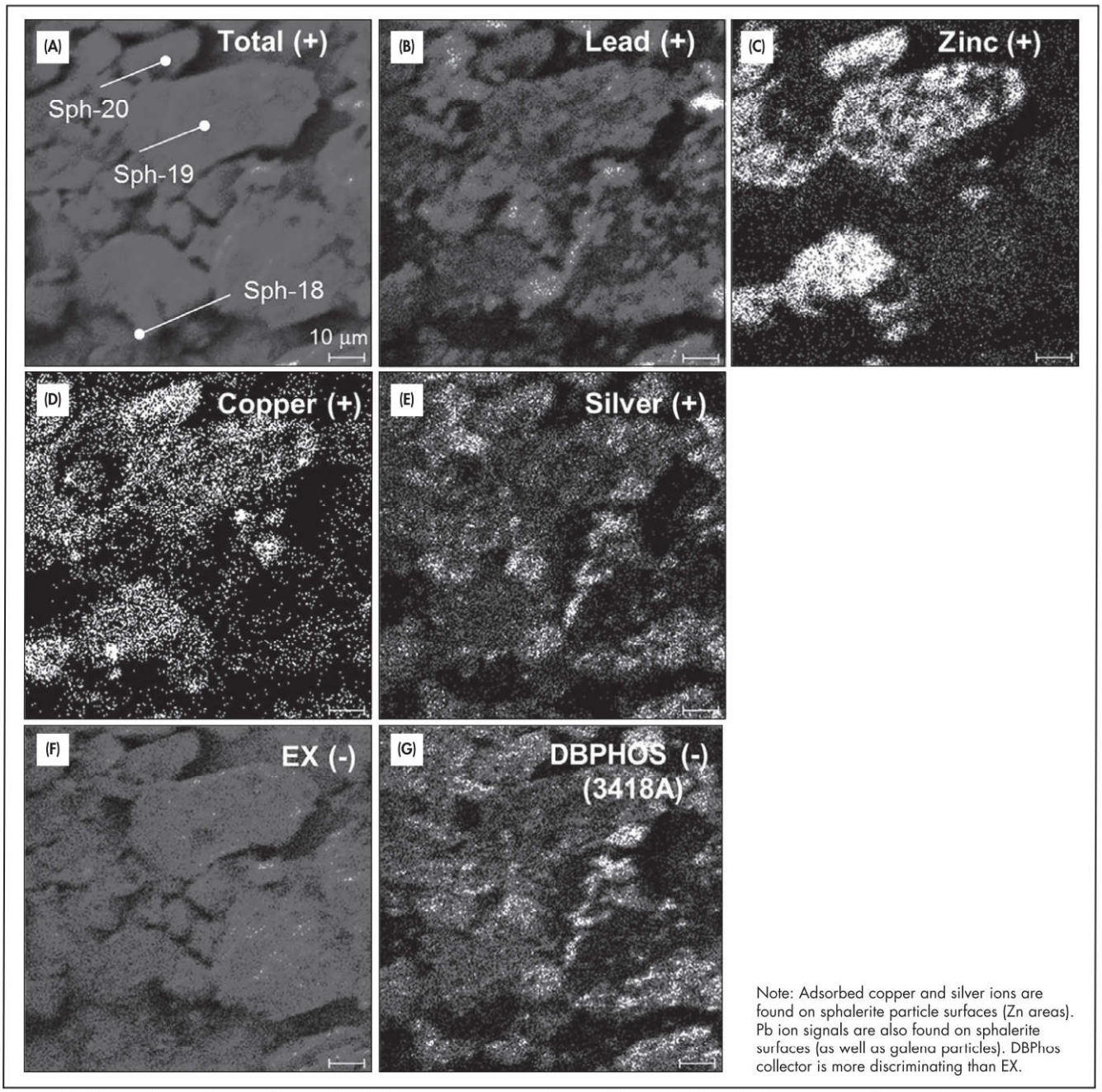

Figure 8 Selected area images from a lead cleaner concentrate for total ion yield, lead, zinc, copper, silver, collector EX, and collector DBPhos

Hence, comparisons show that the surface chemistry of the fine sphalerite is significantly different between concentrates and tails and, for some species, even between the rougher concentrate and scavenger concentrate. The most important difference is the absence of exposure of copper and associated IBX on fine sphalerite in the tail stream, indicating low hydrophobicity of these particles. This difference is exaggerated by the presence of high concentrations of Mg, Ca, Al, OH, and F ions apparently in the form of hydroxides and (alumino)silicates obscuring copper activation. Oxidation to oxy-sulfur species is not a major factor in the depression of fine sphalerite. Calcium ions, in particular, appear to have a depressant role between the rougher and scavenger flotation stages. In the plant, this problem was addressed by improving Ca removal in recycle and staged dosing of Cu down the rougher and scavenger banks.

Non-Sulfide Flotation: Pyrochlore Recovery

In a Niobec mine (Quebec, Canada) plant survey, the composition of the pyrochlore grains reporting to the tails were identified as having a greater concentration of Fe than those reporting to the concentrate. A statistical compositional

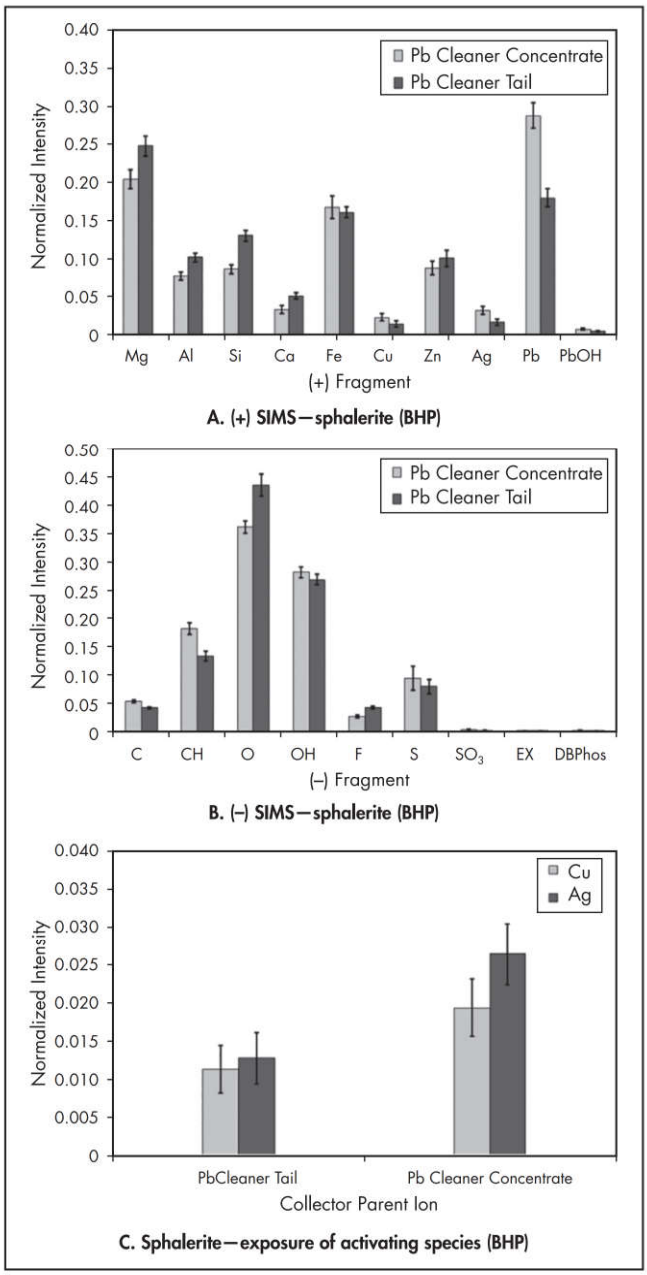

Adapted from Smart et al. 2003b

Figure 9 Statistical comparison of TOF-SIMS normalized intensities for sphalerite particles from a lead cleaner concentrate and tail (bars = 95% confidence intervals) for (A) positive ions, (B) negative ions, and (C) Cu and Ag ions

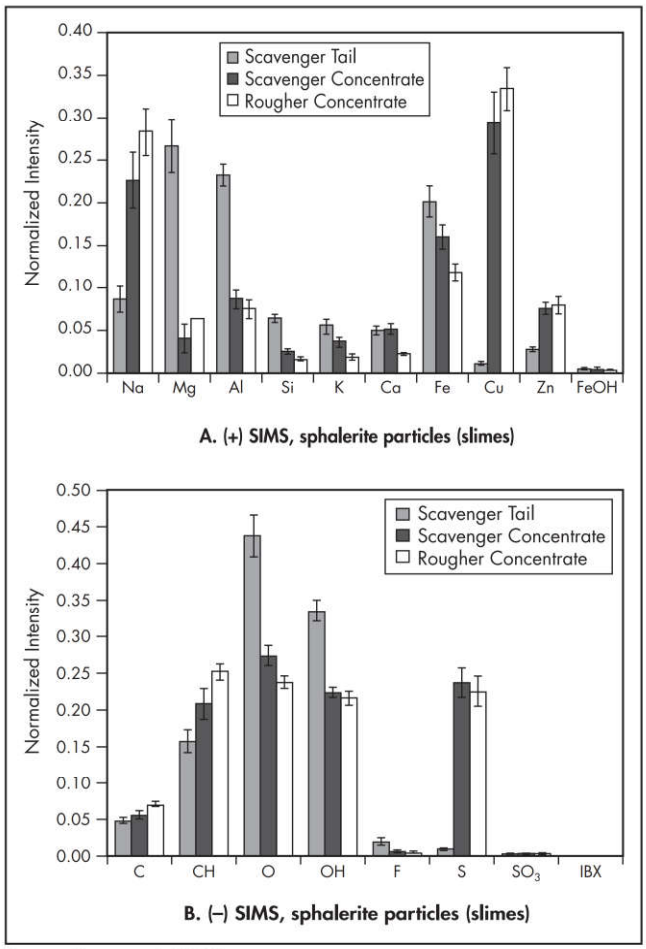

Source: Smart et al. 2003b

Figure 10 Statistical TOF-SIMS spectra for sphalerite particles in the scavenger tail, scavenger concentrate, and rougher concentrate (bars = 95% confidence intervals)

analyses of +200 grains from the concentrate and tails samples showed that the Fe content was not related to Fe-rich inclusions but rather occurred in the mineral matrix, substituting for Na or Ca. TOF-SIMS surface chemical analyses identified that the grains reporting to the tail (higher matrix Fe content) had a greater content of FeOH (along with other FeOx species; Figure 11A) and significantly less tallow diamine (TDM-1) collector on their surfaces (Figure 11B). The TOF-SIMS surface analyses established a link between mineral Fe content, the degree of surface oxidation, collector loading, and the observed poor recovery of high Fe-pyrochlore grains (Chehreh Chelgani et al. 2012a, 2012b).

To verify the relationship between pyrochlore matrix Fe content and the identified surface chemical variations, a series of bench conditioning tests were set up to determine the effect of accelerated oxidation on pyrochlore grains of different Fe content. XPS broad-scan data and high-resolution scans for Fe revealed that, under controlled lab conditions, a greater proportion of oxidative Fe species developed on the surface of the pyrochlore grains with higher matrix Fe content (Chehreh Chelgani et al. 2013, 2014; Figure 11C versus 11D). These data support the hypothesis reached from the TOF-SIMS analyses, which suggest that the development of surface oxides favors pyrochlore grains with higher Fe content, ultimately impeding collector adsorption and reducing recovery.

Rare Earth Element Metals and Minerals

The Nechalacho deposit is a world-class resource of rare earth element (REE) metals and minerals in Canada. Concentration of REEs from the host rocks is accomplished by flotation. In this deposit, heavy rare earth elements (HREEs) are present in fergusonite ((Y, HREE)NbO_4) and zircon ($ZrSiO_4$), whereas the light rare earth elements (LREEs) are present in

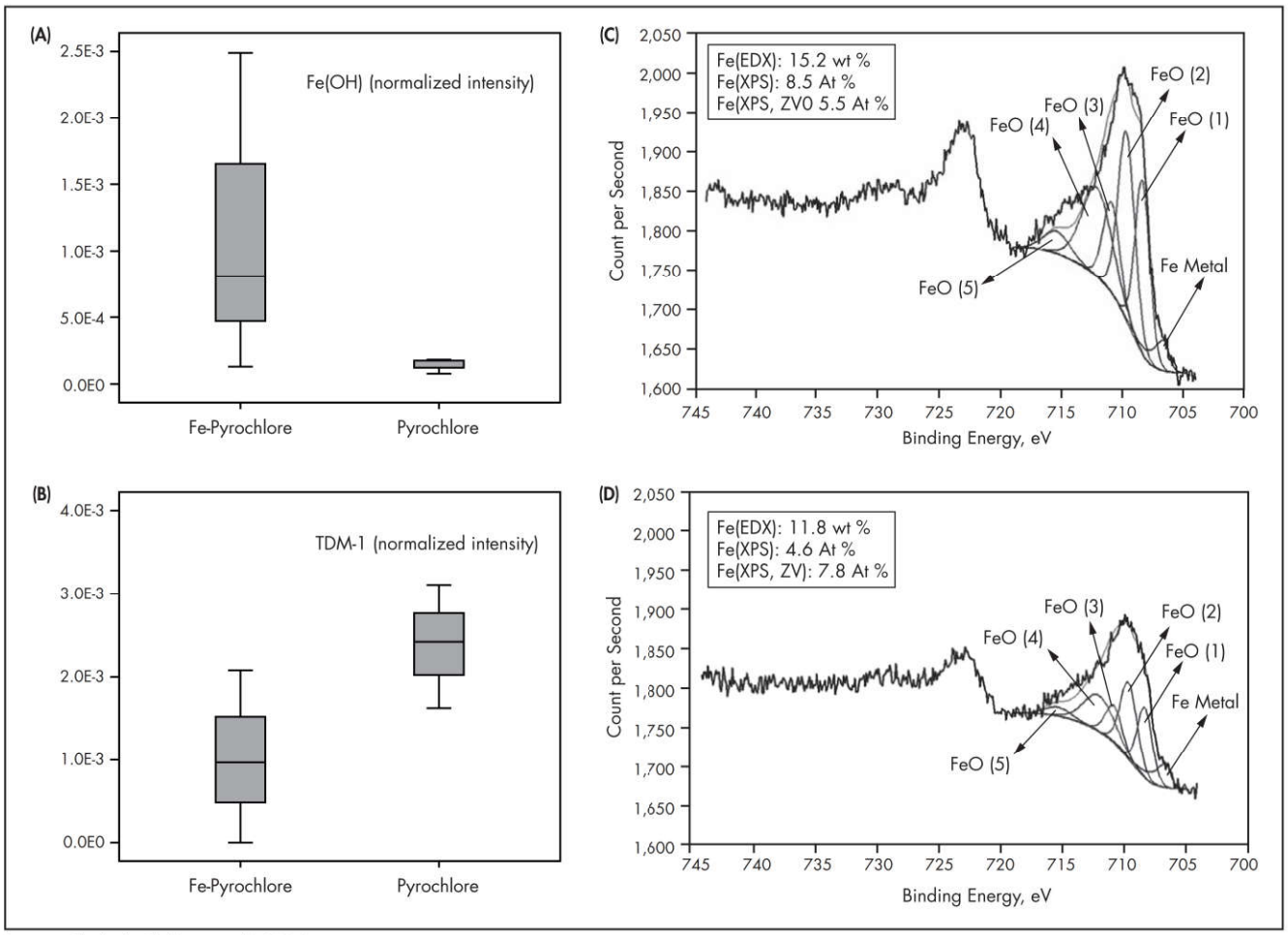

Source: Chehreh Chelgani et al. 2014

Figure 11 (A and B): Vertical box plots of TOF-SIMS normalized intensity for FeOH and collector (TDM-1) on the surface of high Fe pyrochlore (Fe-pyrochlore) and low Fe pyrochlore (pyrochlore) grains from the Niobec flotation plant. (C and D): High-resolution XPS spectra for grains with high Fe content (Fe-pyrochlore, C) versus low Fe content (pyrochlore, D) after conditioning for 30 minutes in O_2-oversaturated water. Included for each grain is the wt % Fe (EDS), the relative atomic proportion (at %) of surface-oxidized FeO components (Fe(XPS)), and Fe metal (ZV-zero valent) proportion of total surface Fe as determined by high-resolution XPS scans.

bastnaesite (Ce, La)CO_3F, synchysite Ca(Y, Ce)$(CO_3)_2F$, allanite (Ce, Ca, Y)$_2$(Al, Fe^{3+})$_3(SiO_4)_3(OH)$, and monazite (Ce, La, Nd, Th)PO_4. Niobium and tantalum are hosted in columbite (Mn, Fe^{2+})$(Nb, Ta)_2O_6$ as well as fergusonite (Paul et al. 2009; Cox et al. 2010).

As part of the development work to optimize a REE mineral recovery process flow sheet, several surface chemical tests tied to the flotation recovery process were used to evaluate the effectiveness and mechanism of hydroxamate adsorption (Xia et al. 2015a, 2015b; Jordens et al. 2013). Laboratory flotation tests revealed that the use of hydroxamates in conjunction with lead nitrate resulted in an obvious improvement in recovery of REE minerals reporting to concentrate. The results suggest that lead nitrate could promote rare earth flotation, but the flotation behavior of each rare earth mineral (REM) is not clear.

The REE flotation grade response results from the Xia et al. (2015a) study in the presence and absence of lead nitrate with benzohydroxamic acid (BHD) as collector is shown in Figure 12. The results with the addition of various doses of lead nitrate ($Pb(NO_3)_2$) show that at low doses (500 g/t or 1,000 g/t), LREE recovery improves significantly, whereas only high doses of lead nitrate (up to 2,000 g/t) result in significant recovery improvements for Zr and Nb. The data imply mineralogical control in flotation recovery of various REMs. Jordens et al. (2013) have identified REE niobates and carbonates as showing the highest recovery rates and REE silicates the lowest. The data from Figure 12 partially supports this contention as La, Ce, Nd, and Y (along with the LREEs) are most commonly found in the easily (fast) recovered carbonate phases in the deposit, whereas Nb and Zr (along with the remainder of the HREEs) are found with the more difficult to recover (slower) oxides and silicates.

In the work by Xia et al. (2015a), surface chemical evaluation of the flotation testing products by TOF-SIMS was performed to potentially identify factors promoting stream partitioning in relation to the addition of $Pb(NO_3)_2$. The surface analysis was performed on samples from flotation tests using 2,000 g/t $Pb(NO_3)_2$ along with the BHD collector. The data show that higher normalized intensities for the BHD

collector (Figure 13) are present on the surface of the grains reporting to the concentrate. The data also show that there is no difference in BHD collector loading rates between the test with and without $Pb(NO_3)_2$ addition, and furthermore, there is no improvement in collector loading discrimination between concentrate and tails grains from the $Pb(NO_3)_2$ addition test. The value of $Pb(NO_3)_2$ then does not appear to be associated with an increase in collector adsorption. The surface chemical data for Pb, on the other hand, shows a strong intensity discrimination on Con/Tail pair grains from the test with the 2,000-g/t $Pb(NO_3)_2$ addition. The intensity data indicate that there is significantly more PbO and PbOH on the surface of the grains reporting to the concentrate than the tails. This would suggest that lead addition can reverse the surface charge, making it more efficient for collectors to adsorb onto REE surfaces. It is also possible that $PbOH^+$ is potentially acting as a point activator for BHD adsorption.

In flotation tests using upgraded REE samples from the same deposit, Jordens et al. (2013) identified similar recovery characteristics using BHD and lead chloride ($PbCl_2$) rather than $Pb(NO_3)_2$. TOF-SIMS surface chemical analyses of REMs showed elevated levels of both PbO and PbOH on the REM grains from the concentrates relative to the tails and that there is selectivity of the Pb species on the REMs over feldspars and Fe-oxides. This greater proportion of PbO and PbOH on grain surfaces from the concentrate would then indicate that $Pb(NO_3)_2$ is indeed participating in the discrimination process and that it may well be providing some degree of selectivity favoring the surface of REM grains.

The ultimate value of both studies was the identification that variability in REE recovery is linked to the flotation characteristics of the various REMs. The recovery process of each

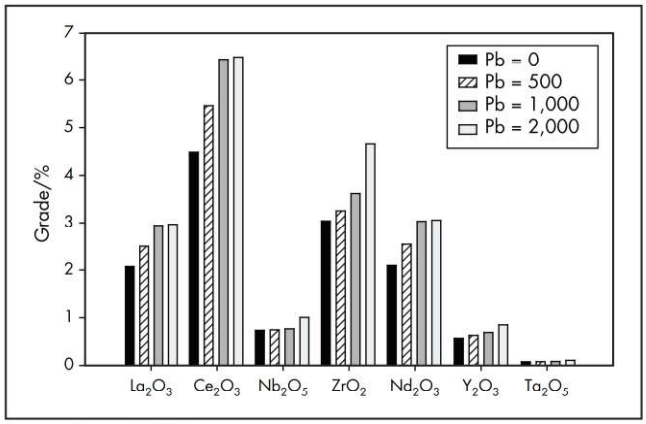

Source: Xia et al. 2015a

Figure 12 Grade of concentrates with different doses (g/t) of Pb as $Pb(NO_3)_2$ using 2,000-g/t BHD as collector

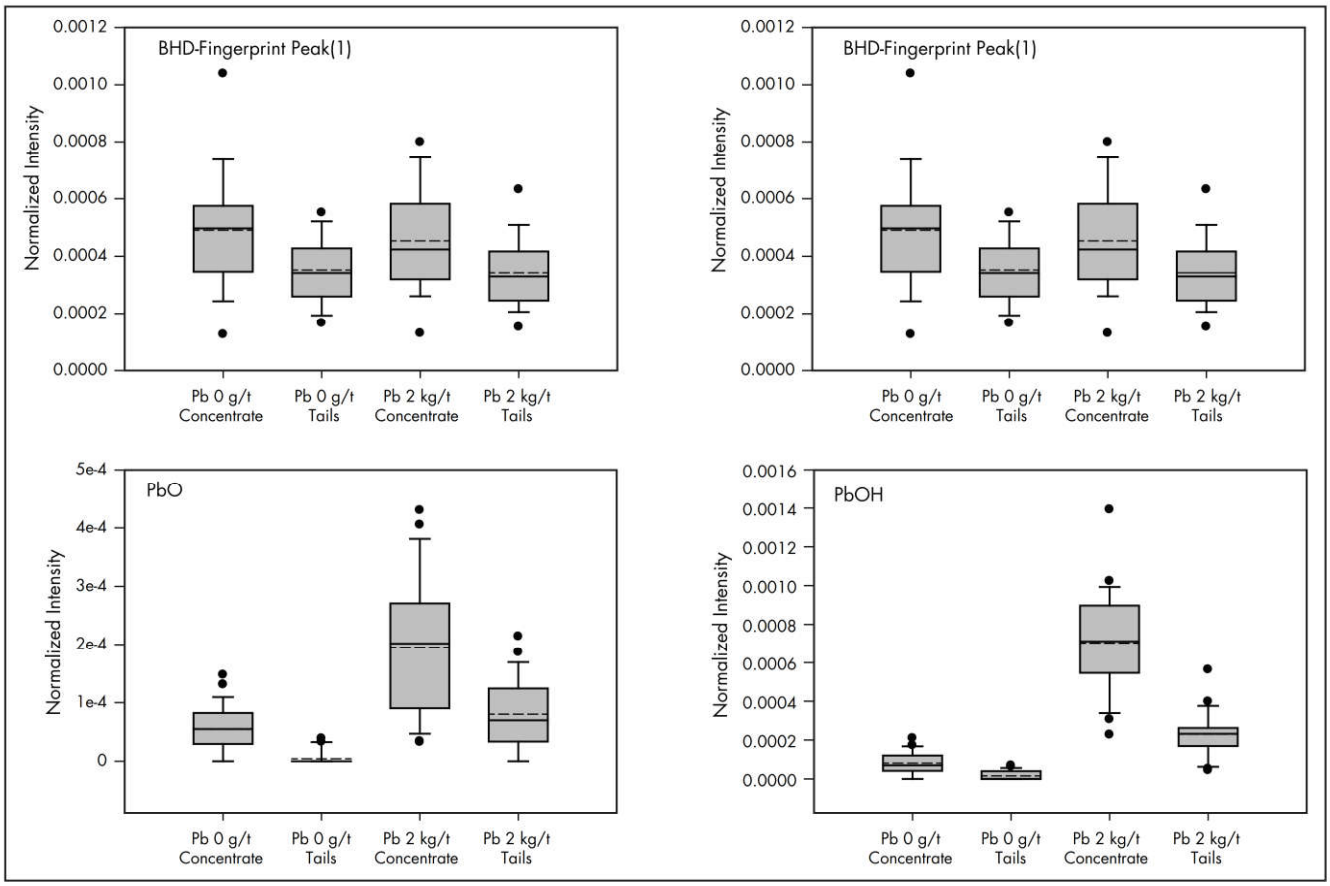

Source: Xia et al. 2015a

Figure 13 Normalized intensity of mass positions indicative of the collectors BHD along with PbO and PbOH on grain surfaces from the control test (no $Pb(NO_3)_2$ addition) and the test with 2,000-g/t $Pb(NO_3)_2$ addition

REE phase is controlled by the interaction of activators and collectors with the mineral surface. The data here indicate that this may well be linked to mineral solubility given that the easily recoverable carbonates are significantly more soluble than the REE silicates. The results of the testing suggest that for the Nechalacho deposit, the most efficient flotation recovery process for the REEs will likely involve a staged addition of both collectors and activators.

Chalcopyrite Leaching

Industrial acid heap and in situ leaching of copper minerals is now used for more than 20% of the world's copper recovery. Copper-containing oxide, hydroxide, sulfate, and silicate minerals acid-leach relatively quickly with Cu(I) oxides (e.g., delafossite and cuprite) being slower. Copper metal and chalcocite-series minerals leach more slowly still with chalcopyrite and bornite being the slowest to leach (Dreier 1999). As chalcopyrite holds approximately 70% of the world's copper reserves, the development of an effective chalcopyrite leach methodology is of considerable industrial interest but has yet to be developed in an economic process.

A considerable number of factors affect leaching rate and cost, including the acid consumption by gangue minerals (e.g., calcite) or, alternatively, acid production through pyrite dissolution. A thorough understanding of bulk mineralogy is therefore vital for calculation of acid balance. This is best approached using more than one technique if the mineralogy is relatively unknown. QEMSCAN and XRD quantitative analyses can be compared directly, but each has its own limitations as described earlier in the "Mineralogy" section. Alternatively, the bulk composition calculated from the mineralogy derived from either of these techniques can be compared to a bulk elemental analysis to check whether there is reasonable agreement.

A further factor that can affect leach rate is galvanic interactions with other minerals. If the rest potential of the value mineral is low as compared to other semiconducting minerals present, then the leach rate will either not be affected or may increase. In this case, the value mineral acts as the anode while the mineral with greater rest potential, often pyrite, acts as the cathode. If the rest potential of the value mineral is greater, leaching may be slowed (Li et al. 2013). The actual physical requirements for galvanic interactions to occur are not yet clear, that is, whether this can happen via solution "contact" or actual physical contact is required. Misdiagnosis of galvanic interaction can occur when leaching gives increased concentrations of Fe^{3+} either directly or via oxidation by O_2 or microbial activity. Importantly, galvanic interactions cease to be a consideration when the solution redox potential becomes greater than the rest potentials of each mineral (e.g., at >660 mV SHE, both pyrite and chalcopyrite will leach independently [Li et al. 2015]).

Solution speciation calculations can be very useful to understanding the behavior of a leach system, but these must be coupled to Eh and pH measurements to evaluate redox pairs—most commonly Fe^{2+}/Fe^{3+} and, in particular, their activity, not overall concentration. It is very common for detailed solution elemental analyses to be done on a regular basis but Eh to never be measured. Solution speciation simulation can be done rapidly and cheaply and is far more accessible than most surface analysis but is seldom carried out. It is not uncommon for an increase in some form of surface speciation or layer formation, most often measured using XPS, to be incorrectly correlated to slow or "passivated" leach kinetics (Crundwell 2013). The most common example of this is the formation of different species in surface layers on chalcopyrite, including polysulfide, elemental sulfur, and iron-containing precipitates (e.g., jarosite [Figure 14]). Although it is not possible to state that surface layer formation is never limiting, many recent studies have suggested otherwise, particularly where leach rates are seen to increase as surface layers are developing and thickening. Particularly if jarosite is present, this would suggest a low solution Fe^{3+} concentration and hence O_2-controlled oxidation, which is considerably slower. In these cases, a focus on solution speciation and gangue mineralogy together with the surface analysis is most valuable.

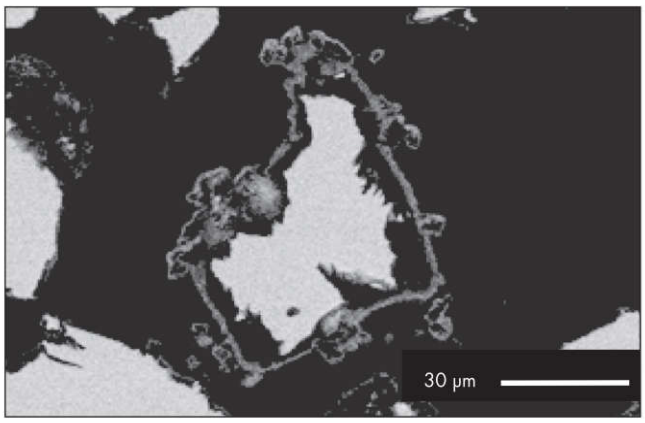

Source: Absolon 2008

A. SEM image of a polished section of chalcopyrite residue from *Sulfolobus metallicus* bioleach after 96 hours (36.5% Cu extraction) showing an unreacted chalcopyrite core surrounded by an S-rich Cu-depleted region containing P and an outer layer rich in Fe containing P and K. Chalcopyrite, sulfur, and spheniscidite were detected by XRD. The leach rate was slow but steady regardless of surface layer buildup.

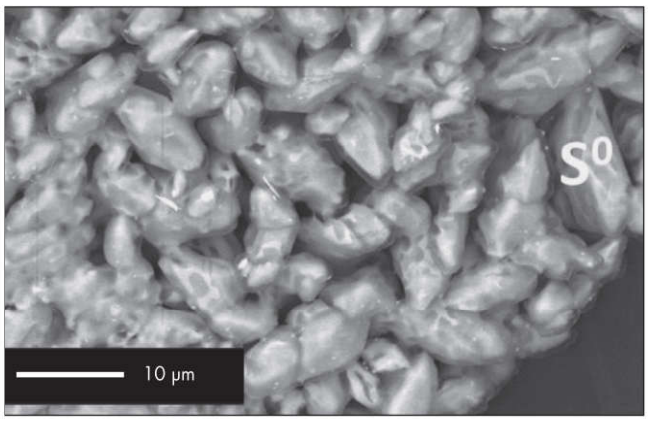

Source: Li et al. 2016

B. SEM image collected from chalcopyrite leached with added 4 mmol iron at 750 mV and 75°C for 72 hours (approximately 100% leached) showing the formation of extensive surface elemental sulfur. The leach rate of the chalcopyrite was very rapid and showed no signs of inhibition.

Figure 14 Examples of non-passivating surface layers

Nickel Laterite Leaching

In contrast to Cu-ore leaching where the value minerals are almost always readily identifiable Cu-minerals, the Ni within nickel laterites is generally present at small concentrations in solid solution across a range of minerals. This complicates the accurate identification of the location of the nickel for process optimization and, importantly, also means that identification of unleached nickel-containing phases can be very difficult.

Because the nickel is not generally present at high concentrations, it is often not detectable using SEM (or QEMSCAN, detection limit typically 1 wt %) but can be quantitatively analyzed using electron probe microanalysis (EPMA). EPMA is similar to EDS as both rely on the measurement of element-specific X-ray fluorescence. EPMA is generally carried out using a small-incident electron beam size, 1−2 µm, and wavelength dispersive spectroscopy, which provide greater spectral resolution than available with EDS. Traditionally, EPMA has been accomplished as a spot analysis on previously identified grains. EPMA-based elemental mapping remains relatively uncommon but has been conducted on nickel laterites (Santos et al. 2015). This analysis is not yet practical on a regular basis, but where identification of losses is crucial, it is a reasonable approach. It is important to remember that this measurement is based on elemental analysis and is not a direct measure of crystallographic structure (i.e., phase), unlike diffraction techniques. Unfortunately, traditional bulk diffraction techniques are not of great use. Although leach residue minerals that may contain Ni can be identified, the precise location of Ni cannot be determined with confidence.

An alternative analytical approach to identify the nature of unleached nickel-containing phases is to use synchtrotron microprobe analysis. Microanalysis may be carried out using diffraction, X-ray fluorescence (XRF), and X-ray adsorption spectroscopy (XAS). XAS enables identification of the local environment around a specific element out to approximately 5 Å. This is useful to understand the location of the nickel within or on a mineral as identified using micro-XRD. A synchrotron provides highly intense X-ray beams that are many orders of magnitude greater than laboratory X-ray sources, enabling analytical approaches otherwise untenable. These facilities, which are widespread around the world, are available to the industry on a user-pays basis or via an experienced collaborator. Although not an approach to be undertaken lightly, the outcomes can be appreciable. For instance, Gerson and Smart undertook XAS analysis of a nickel laterite leach residue from an industrial pilot plant. Identification of the mineralogy of the nickel in the residue enabled process changes to be made, enabling recovery to increase from 70% to 96%. In Fan and Gerson (2015), synchrotron microprobe analyses (XRF, XRD, and XAS) were used to define the nickel mineralogy in saprolite and limonite feeds and leach residues (Figure 15).

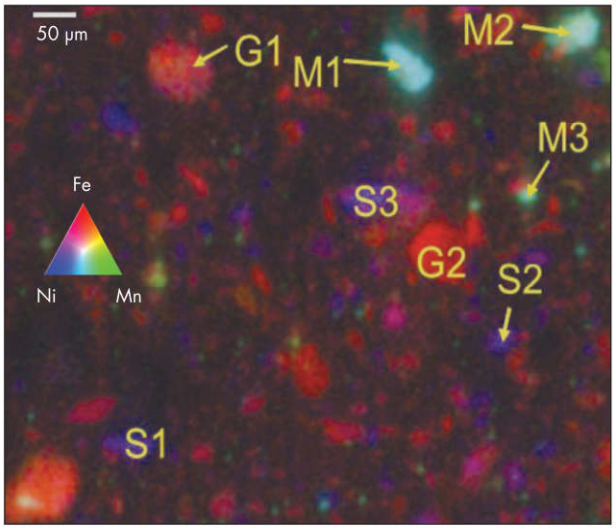

Adapted from Fan and Gerson 2015

A. 600 × 750 µm synchrotron micro-XRF map of a region of a nickel laterite ore showing the distributions of Fe, Ni, and Mn. It is clear that the Ni distribution is highly heterogeneous.

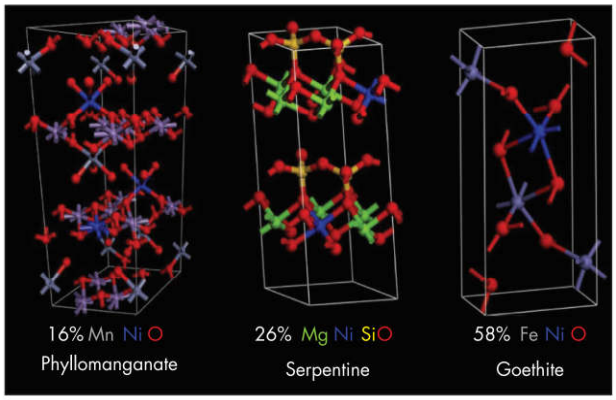

B. Percent location of nickel within the ore. The phase is determined by micro-XRD, and the amount and exact location of the nickel in each crystal structure is derived using micro-XAS analysis.

Figure 15 Location, mineral identification, structure, and distribution of Ni in a nickel laterite ore using synchrotron analysis

Gold Processing: Carbonaceous Matter and Cyanide Leaching

A major obstacle for effective gold recovery during the cyanidation process is the presence of inherent active carbonaceous matter (CM) that has the ability to adsorb, or preg-rob, gold from the cyanide leach solution. Probably the best example is found in the Carlin-type carbonaceous sulfide ores that show varying and significant degrees of preg-robbing activity (Stenebraten et al. 1999; Schmitz et al. 2001; Helm et al. 2009), with excellent reviews on the treatment on preg-robbing ores given by Miller et al. (2005) and Dunne et al. (2013). Many tests are available to determine the preg-robbing capacity of an ore; however, in many instances, the predicted values do not match those of the operating plant. Much of this is due to variability in the nature and presentation of the CM (Hart et al. 2011). In other instances, it may be related to the operation characteristics (pulp chemistry, competing species, etc.). This case study illustrates the combined use of SEM/EDS, TOF-SIMS, and Raman spectroscopy to understand Au losses linked to CM in the ore during the carbon-in-leach (CIL) process. An outline of a procedure where SEM/EDS and Raman spectroscopy, TOF-SIMS, and assays are used to evaluate the preg-robbing capacity of an ore is given in Hart et al. (2011).

The feed to the CIL is a flotation concentrate with upgraded Au values of ≈35 g/t. The CIL residue contained ≈6.5 g/t;

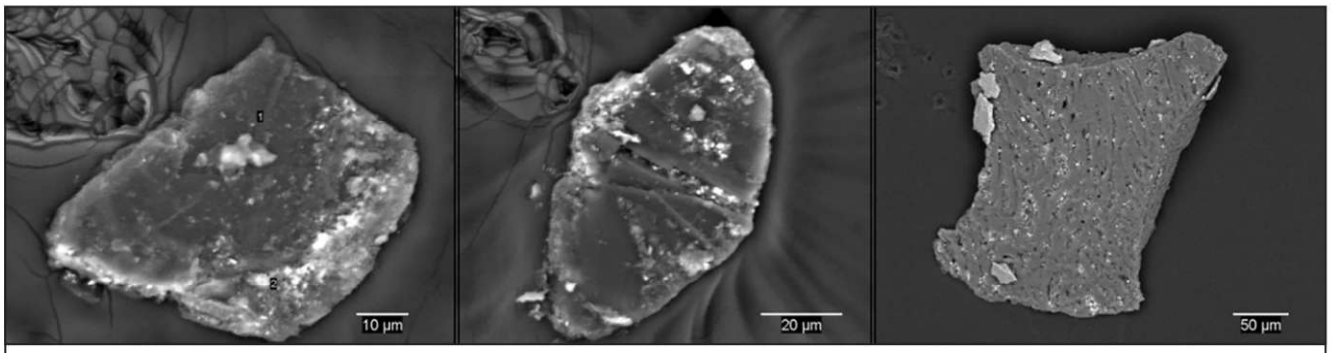

A. Disseminated CM, where the core is CM and the rim on the right side is composed of Si, Al, O, and K with minor Ca and Fe

B. Free CM with small siliceous particles on surface

C. Blocky, coarse, porous CM

Figure 16 BSE images of various forms of CM examined

≈20% of the Au is lost to the tails. The deportment study identified that approximately 10% occurs as locked Au grains and about 20% occurs as invisible Au in sulfides. The remaining lost Au was associated with CM. Detailed SEM/EDS evaluation of the CM in both the CIL feed and leach residue identified both disseminated CM and free CM (Figures 16A and 16B). Also identified were the blocky, porous, coarse grains (Figure 16C). These were only observed in the CIL tails sample.

TOF-SIMS analyses of the CM from the CIL residue (Figure 17) identified gold cyanide Au(CN) on the surface of a significant proportion of the CM grains, verifying that the CM in the sample did indeed preg-rob.

As part of the deportment study, several preg-robbing tests were performed to identify the maximum preg-robbing capacity of the ore. In a geometallurgical context, the measured variability in CM disorder in the ore can be very useful for predicting the preg-robbing response of various blocks to be mined. The degree of disorder of carbon in the CM has been linked to the preg-robbing capacity (Helm et al. 2009)—the less graphitic in nature, the greater the potential to preg-rob.

The CM was analyzed using Raman spectroscopy to determine the internal organization of the carbon (or degree of disorder) and to link this to the degree of preg-robbing. The method of deconvolution of the Raman spectra using the ratios of width (W) to height (H) of the D and G bands is described in Hart et al. 2011 and illustrated for activated carbon in Figure 18A. The rationale for the difference in CM disorder is the significant difference in the saddle height between the D and G bands. The Raman ratio data for the CM from the feed to the CIL process and that from the leach residue of the CIL in this particular case study are given in Figure 18B. Also included on the diagram are the Raman ratios for graphite, activated carbon (from coconut), and the activated carbon that is added to the process for Au recovery. The Raman ratio plot shows two distinct fields: the CIL feed and the CIL residue. The data for the CIL feed samples span the region from graphite to activated carbon, whereas the CIL residue samples show a much greater span and have a significant number of analyses clustered around the Raman ratio for the added activated carbon. The Raman data suggest that many of the carbon grains examined in the CIL residue sample may represent fragments of the carbon added to the process. The SEM/EDS examination of these particular grains shows that their morphology and texture are more representative of activated carbon that supports the interpretation from the Raman analyses.

In the final analyses of the 20% of the Au lost to the tail, slightly more than half of this was due to the inclusion of fragments of added activated carbon; the other half was preg-robbed Au on the inherent "native" carbon within the ore. These fragments of added activated carbon likely result from attrition of the larger chunks added to the CIL process. There is some speculation that the carbon regeneration process may result in a product that is more susceptible to breakage and therefore produces fine particles that are not recovered and are lost to the tails.

RESEARCH AND DEVELOPMENT DIRECTIONS

The current use of these techniques in flotation has been in troubleshooting where plant performance is not meeting targets, has deteriorated unexpectedly, or a change of ore (or stockpile) has occurred. Hence, most analyses have used some of the techniques (e.g., QEMSCAN, SEM, EDTA, TOF-SIMS), but they have not been integrated into the more complete problem-solving strategy (Figure 1). The KUC case study (Gerson et al. 2012; Triffett and Bradshaw 2008; Triffett et al. 2008) provides the model for the most effective use of this technique and information (i.e., where it is correlated to mineralogy, liberation, solution speciation and flotation conditions, and performance with feedback from changes suggested by the results). This is the direction in which development of its application in flotation is proceeding. Practical use of the TOF-SIMS application to process mineralogy has been described in the JKMRC handbook (Smart 2016). Other methods for surface characterization and innovations in research can be found in *Froth Flotation: A Century of Innovation* (Smart et al. 2007) and *Mineral Processing and Extractive Metallurgy: 100 Years of Innovation* (Smart et al. 2014a). Development of the statistical analysis integrated with plant performance is also being pursued within the problem-solving strategy (Gerson and Napier-Munn 2013).

The underutilized areas of development are in application to concentrate and heap leaching operations, where the potential of the full analytical strategy to reveal critical information on the reasons for slow and slowing rates of leaching is considerable, and in extraction processes in gold recovery where interferences can be identified and corrected. It has not yet been used in the statistical analysis mode for these purposes.

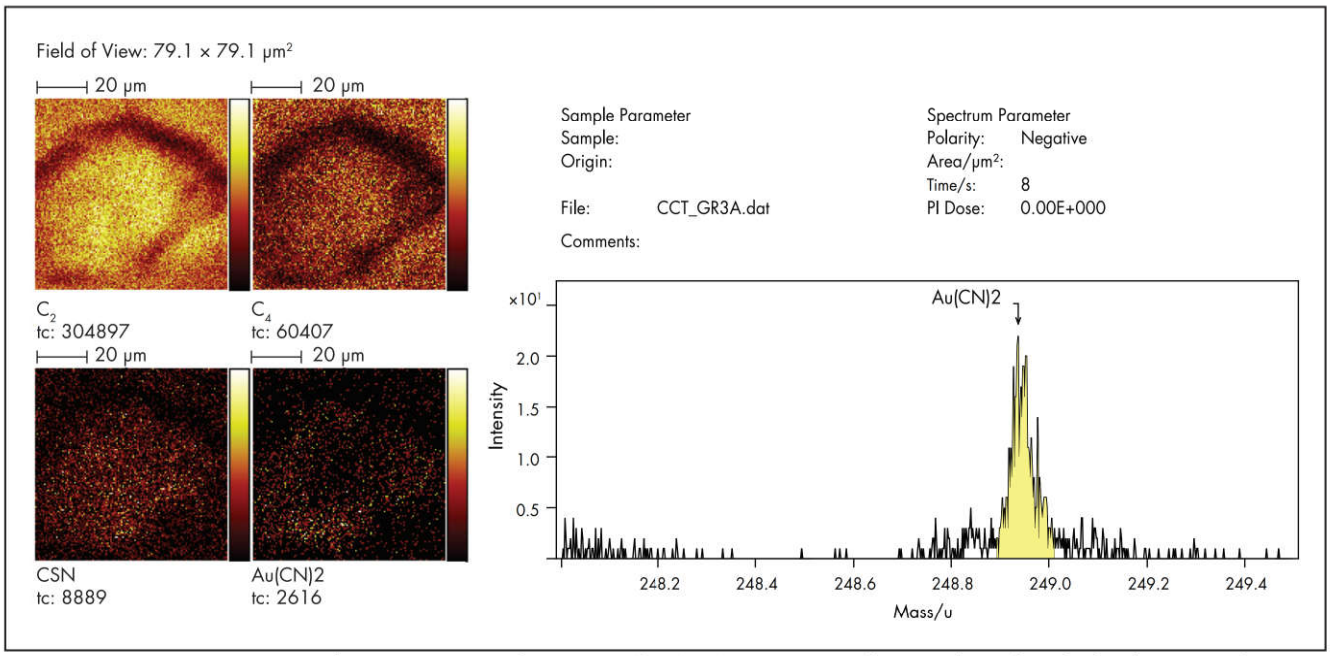

Figure 17 TOF-SIMS images and mass spectra in the region of Au(CN) on CM grain from cyclone classified tailings sample

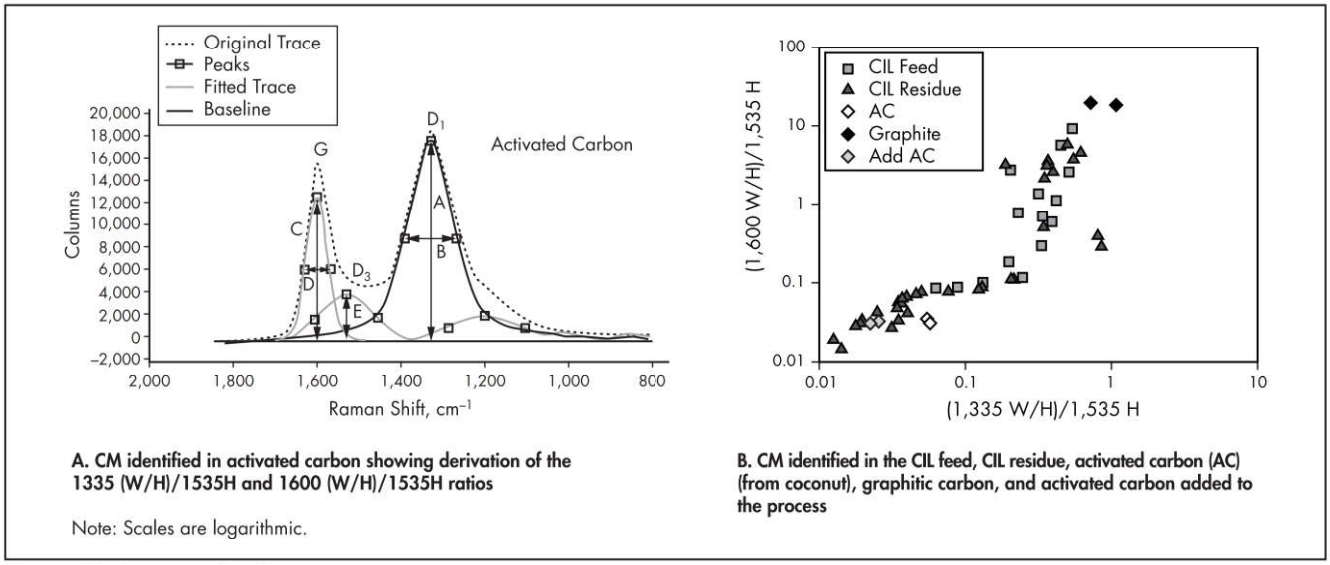

A. CM identified in activated carbon showing derivation of the 1335 (W/H)/1535H and 1600 (W/H)/1535H ratios

B. CM identified in the CIL feed, CIL residue, activated carbon (AC) (from coconut), graphitic carbon, and activated carbon added to the process

Note: Scales are logarithmic.

Figure 18 Raman ratio plots

SUMMARY

Poor flotation recovery or grade and misreporting losses can be caused by poor hydrophobic conditioning of the value mineral surfaces or inadvertent hydrophobic conditioning of gangue mineral surfaces. In leaching operations, interfering solution species, mineral dissolution, and surface layers can limit kinetics and total recovery. To define these limitations, a staged approach can be used to examine mineralogy, solution modeling, oxidation and dissolved metal ion interference, and analytical SEM before it is necessary to examine the surface chemistry in full detail. In addition to MLA and QEMSCAN analysis, losses due to mineralogy (e.g., minor phases, amorphous material, locking at the submicrometer level, and solid solutions) can now be probed using both compositional and diffraction analysis. Finally, however, the hydrophobic/hydrophilic ratio by particle and as a statistical distribution between different mineral phases across a flotation circuit from roughers, scavengers, and cleaners to tail may be needed before changes to mechanical or chemical operation can be effective. Surface analysis using statistical methods in TOF-SIMS can now provide this ultimate information. Direct comparison of intensities and PCA from hydrophobic (principally collectors) and hydrophilic species between feeds, concentrates, and tails can identify surface species discriminating in bubble–particle attachment. These techniques open new opportunities for improvements in recovery and in unrealized value if they are used in plant surveys.

REFERENCES

Absolon, V.J. 2008. A comparison of biological and chemically induced leaching mechanisms of chalcopyrite. PhD thesis, University of South Australia.

Allison, J.D., Brown, D.S., and Novo-Gradac, K.J. 1990. *MINTEQA2/PRODEFA2—A Geochemical Assessment Model for Environmental Systems—Version 3.0 User's Manual.* Athens, GA: Environmental Research Laboratory, Office of Research and Development, U.S. Environmental Protection Agency.

Biesinger, M.C., Polack, R., Hart, B.R., and Kobe, B.A. 2007. Analysis of mineral surface chemistry in flotation separation using imaging XPS. *Miner. Eng.* 20:152–162.

Boulton, A., Fornasiero, D., and Ralston, J. 2003. Characterisation of sphalerite and pyrite flotation samples by XPS and TOF-SIMS. *Int. J. Miner. Process*. 70:205–219.

Brinen, J.S., and Reich, F. 1992. Static SIMS imaging of the diisobutyl dithiophosphinate on galena surfaces. *Surf. Interface Anal.* 18:448–452.

Brinen, J.S., Greenhouse, S., Nagaraj, D.R., and Lee, J. 1993. SIMS and SIMS imaging studies of adsorbed dialkyl dithiophosphinates on PbS crystal surfaces. *Int. J. Miner. Process.* 38:93–109.

Chandra, A.P., and Gerson, A.R. 2006. A review of the fundamental studies of the copper activation mechanisms for selective flotation of the sulfide minerals, sphalerite and pyrite. *Adv. Colloid Interface Sci.* 145:97–110.

Chehreh Chelgani, S., Hart, B., Marois, J., and Ourriban, M. 2012a. Study of pyrochlore surface chemistry effects on collector adsorption by TOF-SIMS. *Miner. Eng.* 39:71–76.

Chehreh Chelgani, S., Hart, B., Marois, J., and Ourriban, M. 2012b. Study of pyrochlore matrix composition effects on froth flotation by SEM-EDX. *Miner. Eng.* 30:62–66.

Chehreh Chelgani, S., Hart, B., and Xia, L. 2013. A TOF-SIMS surface chemical analytical study of rare earth element minerals from micro-flotation tests products. *Miner. Eng.* 45:32–40.

Chehreh Chelgani, S., Hart, B., Biesinger, M., Marois, J., and Ourriban, M. 2014. Pyrochlore surface oxidation in relation to matrix Fe composition: A study by X-ray photoelectron spectroscopy. *Miner. Eng.* 55:165–171.

Chryssoulis, S.L., Reich, F., and Stowe, K.G. 1992. Characterization of mineral surface composition by laser probe microanalysis. *Trans. Inst. Min. Metall. Sect. C* 100:C1–C6.

Chryssoulis, S.L., Weisener, C.G., and Dimov, S. 1995. Detection of mineral collectors by TOF-LIMS. In *Proceedings of Secondary Ion Mass Spectrometry, SIMS X*. Edited by A. Benninghoven, B. Hagenhoff, and H.W. Werner. Chichester: John Wiley and Sons. pp. 899–902.

Coelho Software. 2016. TOPAS-Academic, version 6. Brisbane: Coelho Software.

Cox, J.J., Moreton, Ch., Goode, J.R., and Hains, D.H. 2010. *Technical Report on the Thor Lake Project, Northwest Territories, Canada.* NI 43-101. Toronto, ON: Avalon Rare Metals. pp. 1–350.

Crawford, R., and Ralston, J. 1988. The influence of particle size and contact angle in mineral flotation. *Int. J. Miner. Process*. 23(1-2):1–24.

Crundwell, F.K. 2013. The dissolution and leaching of minerals: Mechanisms, myths and misunderstandings. *Hydrometallurgy* 139:132–148.

Cruz, N., Peng, Y., Farrokhpay, S., and Bradshaw, D. 2013. Interactions of clay minerals in copper–gold flotation: Part 1—Rheological properties of clay mineral suspensions in the presence of flotation reagents. *Miner. Eng.* 50-51:30–37.

Cruz, N., Peng, Y., Wightman, E., and Xu, N. 2015a. The interaction of clay minerals with gypsum and its effects on copper–gold flotation. *Miner. Eng*. 77:121–130.

Cruz, N., Peng, Y., Wightman, E., and Xu, N. 2015b. The interaction of pH modifiers with kaolinite in copper–gold flotation. *Miner. Eng*. 84:27–33.

Dreier, J. 1999. The chemistry of copper heap leaching. http://jedreiergeo.com/copper/article1/Chemistry_of_Copper_Leaching.html.

Dunne, R., Staunton, W.P., and Afewu, K. 2013. A historical review of the treatment of preg-robbing gold ores—What has worked and changed. In *Proceedings of World Gold 2013*. Melbourne, Victoria: Australasian Institute of Mining and Metallurgy. pp. 99–110.

Fan, R., and Gerson, A.R. 2011. Nickel geochemistry of a Philippine laterite examined by bulk and microprobe synchrotron analyses. *Geochim. Cosmochim. Acta* 75:6400–6415.

Fan, R., and Gerson, A.R. 2015. Synchrotron micro-spectroscopic examination of Indonesian nickel laterites. *Am. Mineral.* 100(4):926–934.

Farrokhpay, S., Ndlovu, B., and Bradshaw, D. 2016. Behaviour of swelling clays versus non-swelling clays in flotation. *Miner. Eng.* 96-97:59–66.

Gerson, A.R. 2016. Chapter 14, Synchrotron based process mineralogy techniques. In *Process Mineralogy*. Edited by M. Becker, E.M. Wightman, and C.L. Evans. JKMRC Monograph Series. Indooroopilly, Queensland: Julius Kruttschnitt Mineral Research Centre.

Gerson, A.R., and Jasieniak, M. 2008. The effect of surface oxidation on the Cu activation of pentlandite and pyrrhotite. In *Proceedings of the XXIV International Minerals Processing Congress.* Edited by W.D. Guo, S.C. Yao, W.F. Liang, Z.L. Cheng, and H. Long. Beijing: Science Press. pp. 1054–1063.

Gerson, A., and Napier-Munn, T. 2013. Integrated approaches for the study of real mineral flotation systems. *Minerals* 3(1):1–15.

Gerson, A.R., Lange, A.G., Prince, K.P., and Smart, R.St.C. 1999. The mechanism of copper activation of sphalerite. *Appl. Surface Sci.* 137:207–223.

Gerson, A.R., Smart, R.St.C., Li, J., Kawashima, N., Weedon, D., Triffett, B., and Bradshaw, D. 2012. Diagnosis of the surface chemical influences on flotation performance: Copper sulfides and molybdenite. *Int. J. Miner. Process.* 16:106–109.

Grano, S., Ralston, J., and Smart, R.St.C. 1990. The influence of electrochemical environment on the flotation behaviour of Mt. Isa Mines copper and lead/zinc ores. *Int. J. Miner. Process.* 30:69–97.

Grano, S., Lauder, D.W., Johnson, N.W., and Ralston, J. 1997. An investigation of galena recovery problems in the Hilton concentrator of Mount Isa Mines Limited, Australia. *Miner. Eng.* 10(10):1139–1163.

Greet, C., and Smart, R.St.C. 2002. Diagnostic leaching of galena and its oxidation products with EDTA. *Miner. Eng.* 15:515–522.

Hart, B.R., and Dimov, S.S. 2011. Evolution of ion beam technology towards the needs of the mining and mineral processing industry: A historical Canadian perspective. In *50 Years of COMS.* Edited by J. Kapusta, P. Mackey, and N. Stubina. Westmount, QC: Canadian Institute of Mining, Metallurgy and Petroleum.

Hart, B.R., Dimov, S.S., and Mermillod-Blondin, R. 2011. Procedure for characterization of carbonaceous matter in an ore sample with estimation towards its preg-robbing capacity, World Gold. In *Proceedings of the Conference of Metallurgists: COM 2011*. Montreal, QC: MetSoc. pp. 35–50.

Helm, M., Vaughan, J., Staunton, W.P., and Avraamides, J. 2009. An investigation of carbonaceous component of preg-robbing gold ores. In *World Gold 2009 Conference.* Johannesburg: Southern African Institute of Mining and Metallurgy. pp. 139–144.

Jasieniak, M., and Smart, R.St.C. 2009. Collectorless flotation of pyroxene in Merensky ore: Residual layer identification using statistical TOF-SIMS analysis. *Int. J. Miner. Process*. 92:169–176.

JKTech. 2011. JKSimFloat software. Indooroopilly, Queensland. www.jktech.com.au/jksimfloat.

Johnson, N.W., and Munro, P. 2002. Overview of flotation technology and plant practice for complex sulphide ores. In *Mineral Processing Plant Design, Practice, and Control*. Edited by A.L. Mular, D.N. Halbe, and D.J. Barratt. Littleton, CO: SME. pp. 1097–1123.

Jordens, A., Cheng, Y.P., and Waters, K.E. 2013. A review of the beneficiation of rare earth element bearing minerals. *Miner. Eng.* 41:97–114.

Lastra, R. 2007. Seven practical application cases of liberation analysis. *Int. J. Miner. Process*. 84:337–347.

Li, Y., Kawashima, N., Li, J., Chandra, A.P., and Gerson, A.R. 2013. A review of the structure, and fundamental mechanisms and kinetics of the leaching of chalcopyrite. *Adv. Colloid Interface Sci.* 197-198:1–32.

Li, Y., Qian, G., Li, J., and Gerson, A.R. 2015. Chalcopyrite dissolution at 650 mV and 750 mV in the presence of pyrite. *Metals* 5:1566–1579.

Li, Y., Wei, Z., Qian, G., Li, J., and Gerson, A.R. 2016. Kinetics and mechanisms of chalcopyrite dissolution at controlled redox potential of 750 mV in sulfuric acid solution. *Minerals* 6(3):83.

Madsen, I.C., Scarlett, N.V.Y., and Kern, A. 2011. Description and survey of methodologies for the determination of amorphous content via X-ray diffraction. *Z. Kristallogr.* 226:944–955.

Malysiak, V., Shackleton, N.J., and O'Connor, C.T. 2004. An investigation into the floatability of a pentlandite–pyroxene system. *Int. J. Miner. Process*. 74:251–262.

Miller, J.D., Wan, R.-Y., and Diaz, X. 2005. Preg-robbing gold ores. In *Developments in Mineral Processing*. Vol. 15. Edited by M.D. Adams. Amsterdam: Elsevier. pp. 937–972.

Olsen, C., Makni, S., Hart, B., Laliberty, M., Pratt, A., Blatter, P., and Lanouette, M. 2012. Application of surface chemical analysis to the industrial flotation process of a complex sulphide ore. In *Proceedings of the 26th International Mineral Processing Congress: IMPC 2012.* New Delhi: Indian Institute of Metals.

Owusu, C., Brito e Abreu, S., Skinner, W., Addai-Mensah, J., and Zanin, M. 2014. The influence of pyrite content on the flotation of chalcopyrite/pyrite mixtures. *Miner. Eng.* 55:87–95.

Parolis, L.A.S., van der Merwe, R., van Leerdam, G.C., Prins, F.E., and Smeink, R.G. 2007. The use of TOF-SIMS and microflotation to assess the reversibility of CMC binding onto talc. *Miner. Eng.* 20:970–978.

Paul, J., Stubens, T.C., Arseneau, G., and Maunula, T. 2009. *Avalon Rare Metals Inc. Thor Lake—Lake Zone Mineral Resource Update.* Toronto, ON: Avalon Rare Metals. pp. 1–193.

Peng, Y., Bo, W., and Gerson, A. 2012. The effect of electrochemical potential on the activation of pyrite by copper and lead ions during grinding. *Int. J. Miner. Process.* 102:141–149.

Piantadosi, C., and Smart, R.St.C. 2002. Statistical comparison of hydrophobic and hydrophilic species on galena and pyrite particles in flotation concentrates and tails from TOF-SIMS evidence. *Int. J. Miner. Process.* 64:43–54.

Piantadosi, C., Jasieniak, M., Skinner, W.M., and Smart, R.St.C. 2000. Statistical comparison of surface species in flotation concentrates and tails from TOF-SIMS evidence. *Miner. Eng*. 13:1377–1394.

Ralston, J., and Healy, T.W. 1980. Activation of zinc sulphide with Cu^{II}, Cd^{II} and Pb^{II}: II. Activation in neutral and weakly alkaline media. *Int. J. Miner. Process.* 7(3):203–217.

Ralston, J., Fornasiero, D., and Grano, S. 2007. Pulp and solution chemistry. In *Froth Flotation: A Century of Innovation*. Edited by M.C. Fuerstenau, G. Jameson, and R.-H. Yoon. Littleton, CO: SME. pp. 227–258.

Santos, R.M., Audenaerde, A.V., Chiang, Y.W., Iacobescu, R.I., Knops, P., and Van Gerven, T. 2015. Nickel extraction from olivine: Effect of carbonation pre-treatment. *Metals* 5:1620–1644.

Saxby, J.D., and Stephens, J.F. 1973. Carbonaceous matter in sulphide ores from Mount Isa and McArthur River: Ark investigation using the electron probe and electron microscope. *Miner. Depositor* 8:127–137.

Schmitz, P.A., Duyvesteyn, S., Johnson, W.P., Enloe, L., and McMullen, J. 2001. Ammoniacal thiosulfate and sodium cyanide leaching of preg-robbing goldstrike ore carbonaceous matter. *Hydrometallurgy* 60(1):25–40.

Shackleton, N.J., Malysiak, V., and O'Connor, C.T. 2007. Surface characteristics and flotation behaviour of platinum and palladium arsenides. *Int. J. Miner. Process.* 85(1):25.

Shaff, J.O., Schultz, B.A., Craft, E.J., Clark, R.T., and Kochian, L.V. 2010. GEOCHEM-EZ: A chemical speciation program with greater power and flexibility. *Plant Soil* 330(1-2):207–214.

Smart, R.St.C. 2016. Chapter 12, Time of flight secondary ion mass spectrometry. In *Process Mineralogy.* Edited by M. Becker, E.M. Wightman, and C.L. Evans. JKMRC Monograph Series. Indooroopilly, Queensland. pp. 149–161.

Smart, R.St.C., Amarantidis, J., Skinner, W.M., Prestidge, C.A., LaVanier, L., and Grano, S.G. 2003a. Surface analytical studies of oxidation and collector adsorption in sulfide mineral flotation. In *Solid–Liquid Interfaces.* Topics in Applied Physics series, Vol. 85. Edited by K. Wandelt and S. Thurgate. Berlin: Springer-Verlag. pp. 3–60.

Smart, R.St.C., Jasieniak, M., Piantadosi, C., and Skinner, W.M. 2003b. Diagnostic surface analysis in sulfide flotation. In *Flotation and Flocculation: From Fundamentals to Applications*. Edited by J. Ralston, J.D. Miller, and J. Rubio. Adelaide: Ian Wark Research Institute, University of South Australia. pp. 241–248.

Smart, R.St.C., Skinner, W.M., Gerson, A.R., Mielczarski, J., Chryssoulis, S., Pratt, A.R., Lastra, R., Hope, G.A., Wang, X., Fa, K., and Miller, J.D. 2007. Surface characterization and new tools for research. In *Froth Flotation: A Century of Innovation*. Edited by M.C. Fuerstenau, G. Jameson, and R.-H. Yoon. Littleton, CO: SME. pp. 283–338.

Smart, R.St.C, Gerson, A.R., Hart, B.R., Beattie, D.R., and Young, C. 2014a. Innovations in measurement of mineral structure and surface chemistry in flotation: past, present and future. In *Mineral Processing and Extractive Metallurgy: 100 Years of Innovation.* Edited by C.G. Anderson, R.C. Dunne, and J.L. Uhrie. Englewood, CO: SME. pp. 577–602.

Smart, R.St.C., Xu, N., Fan, R., and Gerson, A.R. 2014b. A strategic approach to flotation losses due to mineralogy and surface chemistry. In *Proceedings of the XXVII International Mineral Processing Congress 2014: IMPC 2014.* Santiago, Chile: IMPC. pp. 1–12.

Stenebraten, J.F., Johnson, W.P., and Brosnahan, D.R. 1999. Characterization of Goldstrike ore carbonaceous material. *Miner. Metall. Process.* 16(3):37–43.

Stowe, K.G., Chryssoulis, S.L., and Kim, J.Y. 1995. Mapping of composition of mineral surfaces by TOF-SIMS. *Miner. Eng.* 8(4-5):421–430.

Sui, C.C., Lee, D., Casuge, A., and Finch, J.A. 1999. Comparison of the activation of sphalerite by copper and lead ions. *Miner. Metall. Process.* 16(2):53–61.

Toran, L., and Grandstaff, D. 2002. PHREEQC and PHREEQCI: Geochemical modeling with an interactive interface. *Ground Water* 40:462–464.

Trahar, W.J. 1976. The selective flotation of galena from sphalerite with special reference to the effects of particle size. *Int. J. Miner. Process.* 3:151–166.

Triffett, B., and Bradshaw, D. 2008. The role of morphology and host rock lithology on the flotation behaviour of molybdenite at Kennecott Utah Copper. In *Ninth International Congress for Applied Mineralogy: ICAM 2008*. Melbourne, Victoria: Australasian Institute of Mining and Metallurgy. pp. 465–473.

Triffett, B., Veloo, C., Adair, B.J.I., and Bradshaw, D. 2008. An investigation of the factors affecting the recovery of molybdenite in the Kennecott Utah Copper bulk flotation circuit. *Miner. Eng.* 21(12-14):832–840.

Tukel, C., Kelebek, S., and Yalcin, E. 2010. Eh-pH stability diagrams for analysis of polyamine interaction with chalcopyrite and deactivation of Cu-activated pyrrhotite. *Can. Metall. Q.* 49:411–418.

Xia, L., Hart, B., and Loshusan, B. 2015a. A TOF-SIMS analysis of the effect of lead nitrite on rare earth flotation. *Miner. Eng.* 70:119–129.

Xia, L., Hart, B., Douglas, K., and Zhong, H. 2015b. Two new structures of hydroxamate collectors and their application to ilmenite and wolframite flotation. In *Proceedings of the 47th Annual Meeting of the Canadian Mineral Processors*. Westmount, QC: Canadian Institute of Mining, Metallurgy and Petroleum. pp. 185–193.

Xu, N., Fan, R., and Smart, R.St.C. 2014. Cryo-SEM investigation of aggregate structures of clay minerals in flotation pulp and froth. In *Proceedings of the XXVII International Mineral Processing Congress 2014: IMPC 2014.* Santiago, Chile: IMPC. pp. 1–11.

Zhang, M., and Peng, Y. 2015. Effect of clay minerals on slurry rheology and the flotation of copper and gold minerals. *Miner. Eng*. 70:8–13.